

Supporting information to

The UWO dataset – long-term observations from a full-scale field laboratory to better understand urban hydrology at small spatio-temporal scales

Frank Blumensaat^{1,2,3}, Simon Bloem¹, Christian Ebi¹, Andy Disch¹, Christian Förster¹, Mayra Rodriguez¹, Max Maurer^{1,2}, Jörg Rieckermann^{1*}

¹Department of Urban Water Management, Eawag, Swiss Federal Institute of Aquatic Science and Technology, 8600 Dübendorf, Switzerland

²Institute of Civil, Environmental and Geomatic Engineering, ETH Zürich, 8093, Zurich, Switzerland

³Landesdirektion Sachsen, Stauffenbergallee 2, 01099 Dresden, Germany

Contents

S1	Climatology	6
S1.1	Overview.....	6
S1.2	Fundamentals.....	6
S1.3	Water in the Atmosphere.....	7
S1.4	Water on the Earth's surface	7
S1.5	Water in the Lithosphere	8
S1.6	Extreme Point precipitation	9
S2	Flow scheme and subcatchments characteristics	10
S2.1	The drainage system	10
S2.2	Municipal water use, wastewater characteristics and sewer infiltration	13
S3	Stormwater treatment and flow control structures.....	14
S3.1	Overview on hydraulic network structures.....	14
S3.2	Stormwater treatment facility <i>RUB Morgenthal</i>	16
S3.3	In-sewer storage facility <i>FK 102 (FK Stadacher)</i>	17
S3.4	Stormwater treatment facility <i>RUB 128 (RUB Usterstrasse)</i>	18
S3.5	Stormwater treatment facility <i>RUB 59 (RUB ARA)</i>	19
S3.6	RUB PW80 (RUB Industrie).....	20
S3.7	Flow splitting structure <i>VS600</i>	21
S3.8	Flow splitting structure <i>VS 22</i>	22
S3.9	Flow control structure <i>RU 40a</i>	23

S3.10	In-sewer flow distribution facility <i>US 58</i>	24
S3.11	Stormwater overflow <i>RU 48b</i> (emergency overflow)	25
S4	Sensor classes	26
S4.1	Rain gauge: <i>RM Young 52202</i>	26
S4.2	Rain gauge: <i>Ott Pluvio 2L</i>	27
S4.3	Water level: <i>Maxbotix MB 7389/7369</i>	28
S4.4	Capacitive overflow detection: <i>Meter 5TM</i>	29
S4.5	Temperature: <i>dual temperature sensors</i>	30
S4.6	Flow and velocity: <i>Flo-Dar, Marsh-MCBirney</i>	31
S4.7	Flow and velocity: <i>Sommer SQ-3</i>	32
S4.8	Flow and velocity: <i>NIVUS POA/CSM sensor</i>	33
S4.9	Weather and climate: <i>SHT-21/35</i>	34
S4.10	Water level: <i>Keller 36KyX</i>	35
S4.11	Data transmission: <i>LoRa-based mesh system</i>	36
S4.12	Utility routine monitoring - PLS data.....	37
S4.13	Weather monitoring station <i>Lufft WS-700</i>	38
S4.14	Other sensors	39
S4.15	Gateways	40
S5	Data storage and management in the “Datapool” warehouse	41
S5.1	The “Datapool” data warehouse.....	41
S5.2	General definitions used in the Datapool	41
S5.3	Source-ID-naming conventions in the UWO Datapool.....	41
S5.3.1	General rules for source ID nomenclature.....	41
S5.3.2	Nomenclature for <i>source ID’s</i>	42
S5.4	Attributes for meta-data entries	43
S5.5	Revised data model for <i>Datapool 2.0</i>	45
S5.6	Tracking issues in the UWO dataset using a version control system	49
S6	Dynamic plot of the data completeness.....	50
S7	Hydrodynamic sewer models	51
S7.1	Hydrodynamic sewer modelling.....	51
S7.2	Sewer network implementation in EPA SWMM	51
S7.3	Adjustment of the SWMM model to observations	53
S7.4	Past and current developments of the SWMM model	55
S8	Exploring operational challenges: lessons from operating a full-scale field laboratory for urban drainage monitoring	57
S8.1	Co-operation with the municipal utility and communication with the public.....	57
S8.2	Internal collaboration, knowledge management and work safety	57

S8.3	Sewer monitoring equipment, sensor choice and the challenge of maintaining good data quality	58
S8.4	The importance of metadata.....	59
S8.5	Telecommunication and data transmission	60
S9	Research opportunities	61
S9.1	Anomaly detection of sewer monitoring data using semi-automated machine learning approaches	61
S9.2	Quantification of groundwater infiltration	63
S9.3	The value of redundant sensors in event-duration monitoring.....	65
S9.3.2	Results	66
S9.3.3	Conclusion	68
S9.4	The performance of a LoRaWAN network for underground applications.....	69
S10	References.....	71

Figure S1. Figure 1..... **Error! Bookmark not defined.**

S1 Climatology

S1.1 Overview

Climatological data are openly available for Switzerland from the Hydrological Atlas of Switzerland (HADES). HADES is a joint effort from Swiss hydrologic organizations, i.e. federal departments, and cantons as well as research establishments and private water sector experts. For three decades it has been providing essential hydro knowledge, specific know-how and educational materials to an extensive range of consumers. The Atlas consists in the original selection of 63 printed charts plus multiple other more recent products that can be accessed through the hydrological atlas of Switzerland¹.

The following information has been compiled from the webapp *hydromaps.ch*. The presented catchment characteristics for the Fehraltorf catchment (ID: 134760²) follow the presentation in the webapp.

S1.2 Fundamentals

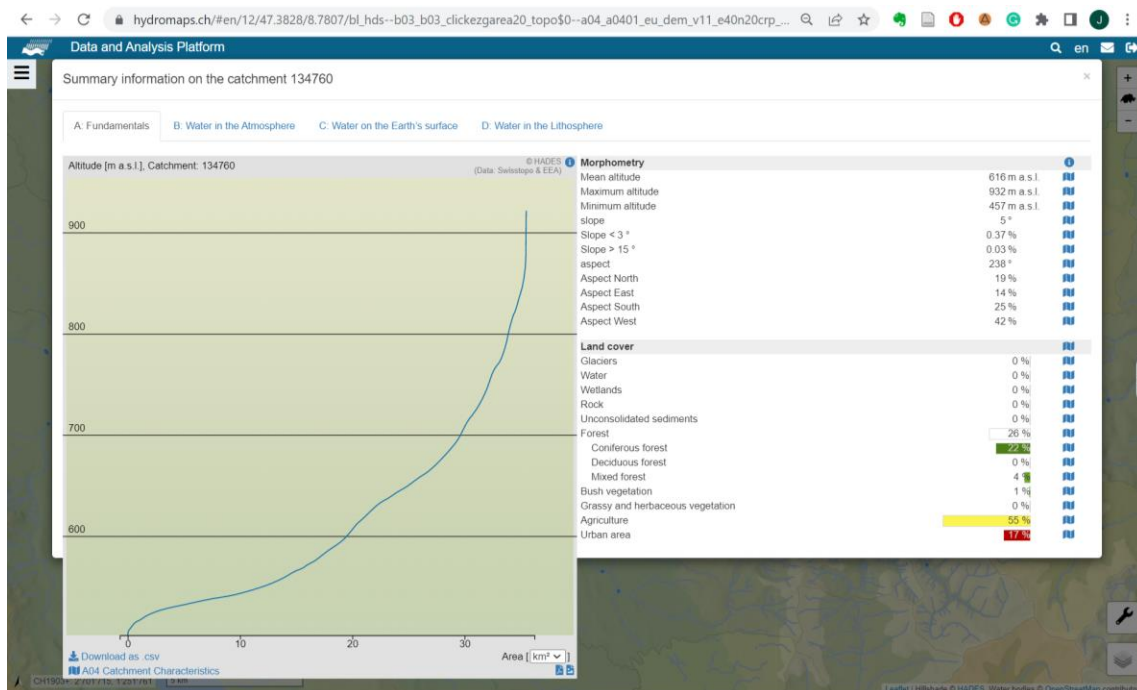


Figure S 1: Data on fundamental characteristics, such as morphology, etc. from www.hydromaps.ch. © HADES .Water bodies © OpenStreetMap3 contributors 2024. Distributed under the Open Data Commons Open Database License (ODbL) v1.0.

¹ <https://hydrologischeratlas.ch/>

² [https://hydromaps.ch/#en/12/47.3828/8.7807/bl_hds--b03_b03_clickezgarea20_topo\\$0--a04_a0401_eu_dem_v11_e40n20crp_chv1_0\\$0/134760+3](https://hydromaps.ch/#en/12/47.3828/8.7807/bl_hds--b03_b03_clickezgarea20_topo$0--a04_a0401_eu_dem_v11_e40n20crp_chv1_0$0/134760+3) (accessed on 15.1.2024)

³ <https://www.openstreetmap.org/>

S1.3 Water in the Atmosphere

Summary information on the catchment 134760

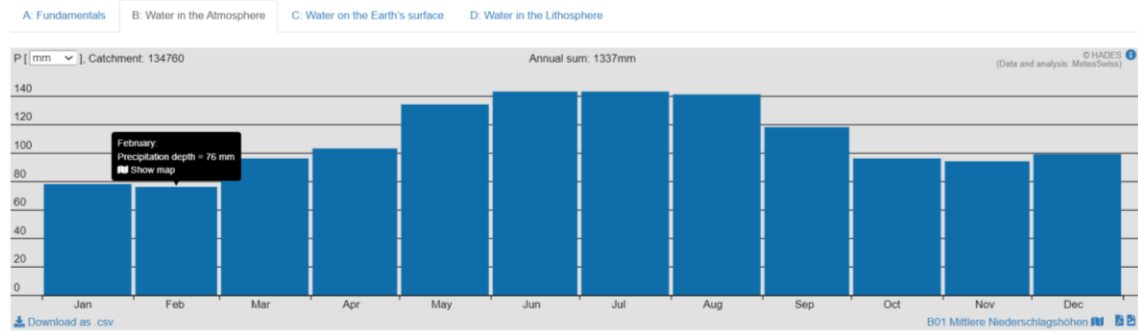


Figure S 2: Long-term mean of monthly precipitation depths, in mm

S1.4 Water on the Earth's surface

Summary information on the catchment 134760

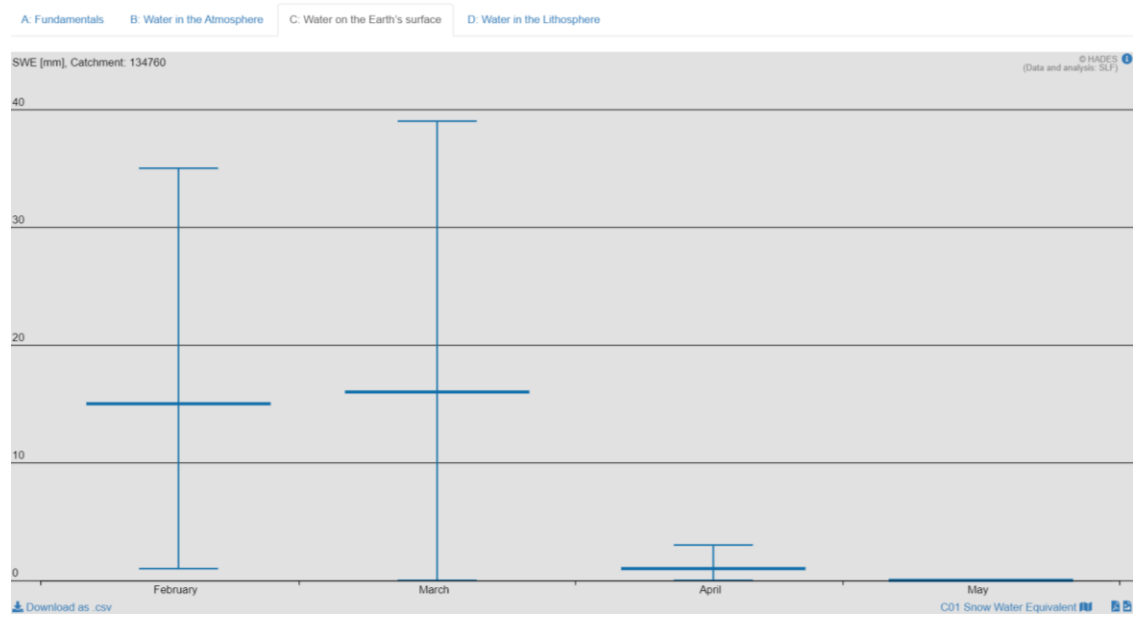


Figure S 3: Snow-Water equivalent (SWE) in the Fehraltorf catchment

S1.5 Water in the Lithosphere

Summary information on the catchment 134760

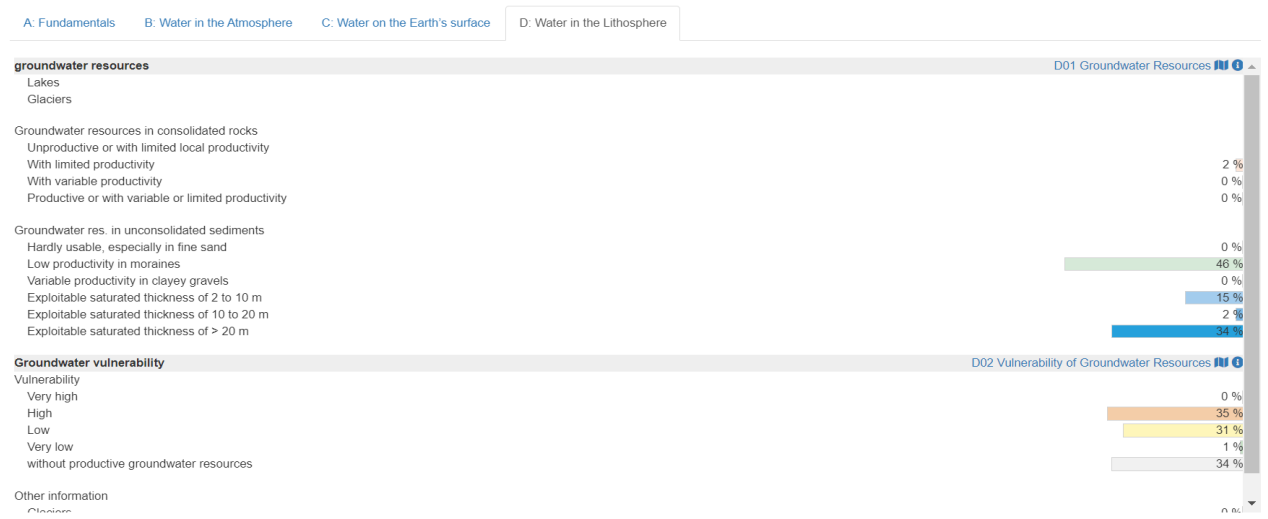


Figure S 4: Groundwater resources and vulnerability

S1.6 Extreme Point precipitation

The information on "Extreme Point precipitation" (Figure S 5) shows precipitation levels for exceptionally heavy rainfall events that may transpire within a span of 2 to 200 years. At present, findings are available for both 24-hour and one-hour rain accumulations. In due course, assessments for additional timeframes will be accessible as well. Each segment on this map is accompanied by a table providing median values along with their uncertainty ranges at the center point of each section. The color gradient varies according to distinct return periods and duration stages. To accurately interpret these maps while considering potential constraints outlined in Frei et al. (2018)⁴, it's essential to keep them in mind when examining the data presented herein.

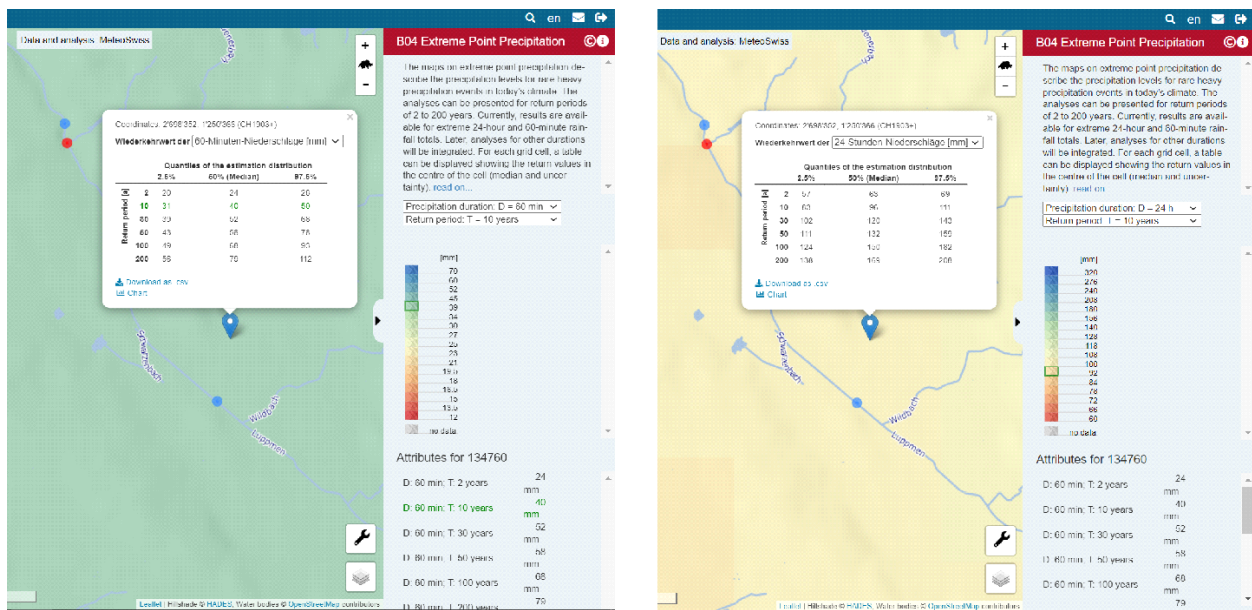


Figure S 5: Extreme point precipitation in Fehraltorf for durations of 60min (left) and 24 hours (right), based on Frei et al. (2022)⁵. © HADES .Water bodies © OpenStreetMap⁶ contributors 2024. Distributed under the Open Data Commons Open Database License (ODbL) v1.0 (both Figures).

⁴ Christoph Frei, Francesco A. Isotta, Jan Schwanbeck (2018). "Mean Precipitation 1981–2010". In Data and Analysis Platform. Hydrological Atlas of Switzerland.

⁵ Christoph Frei, Sophie Fukutome (2022). "Extreme Point Precipitation". In Data and Analysis Platform. Hydrological Atlas of Switzerland. https://hydromaps.ch/#en/8/46.830/8.190/bl_hds--b04_b0401_precip_60m_2a_0_5v2_054/NULL (accessed on 20.03.2023).

⁶ <https://www.openstreetmap.org/>

S2 Flow scheme and subcatchments characteristics

S2.1 The drainage system

The municipal wastewater and stormwater in Fehraltorf are collected through a combined sewer network and conveyed to the central wastewater treatment plant (WWTP). Gravity facilitates sewage flow in the primary part of the catchment, while in a small subcatchment southwest of the city center, combined sewage is pumped. The simplified hydrological scheme in (Figure S 6) illustrates the primary flow path and features of the main retention and overflow facilities. The primary collector follows the designated slope in the catchment, passing through hydraulic structures such as VS600, VS22 (flow splitters), RUB128 (retention basin), and US58 (in-sewer overflow). Originating from the upper periphery in the Northeast (Russikon), waste- and stormwater travel to the central WWTP at the lower southeast end. Additionally, the system receives two substantial transfer flows from neighbouring municipalities in the North, namely Rumlikon and Russikon.

The sewer network topology is rather simple: a fishbone-like structure with two inner loops at which flow splitters allow wastewater to travel into different directions, but only during intense rain weather periods. Dry weather flow times for main collector sections are estimated within the scope of the Urban Drainage Master Planning (HBT, 2016).

The system includes the following hydraulic structures: three stormwater treatment facilities with retention volume, one interceptor sewer, six combined sewer overflows without retention volume and several flow splitting structures. There are very few manually controllable flow limiters in the system: a vortex throttle at RUB Morgenthal, and a pipe throttle limiting the inflow to the WWTP. The system's operation is ensured by manual control, there is no real-time control scheme in place.

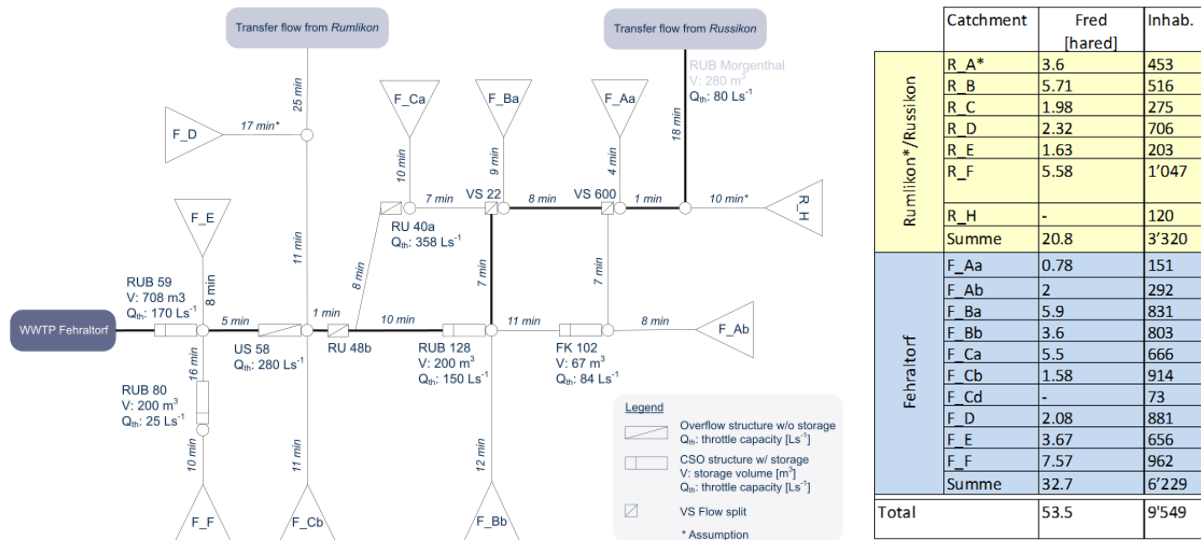


Figure S 6: Flow topology (left) and aggregated information on the subcatchments (right).

Fundamental information provided in the Urban Drainage Master Plans VGEP⁷ Fehrltorf-Russikon (HBT, 2014) and GEP⁸ Fehrltorf (HBT, 2016) were used as basis for studies in the scope in the UWO project. The GEP 2014 contains information on size and characteristics of subcatchment such including discharge coefficients and population densities per building zone. Current and expected changes due to urban development have been taken into account in the VGEP from 2014 (HBT, 2014) according to the current zoning plan (state 2014), where an increase in building density (10 %) and an increase in population density (15 %) are expected. Hydrological key figures, such as the area that produces runoff and population densities were increased accordingly (cf. Figure S 7).

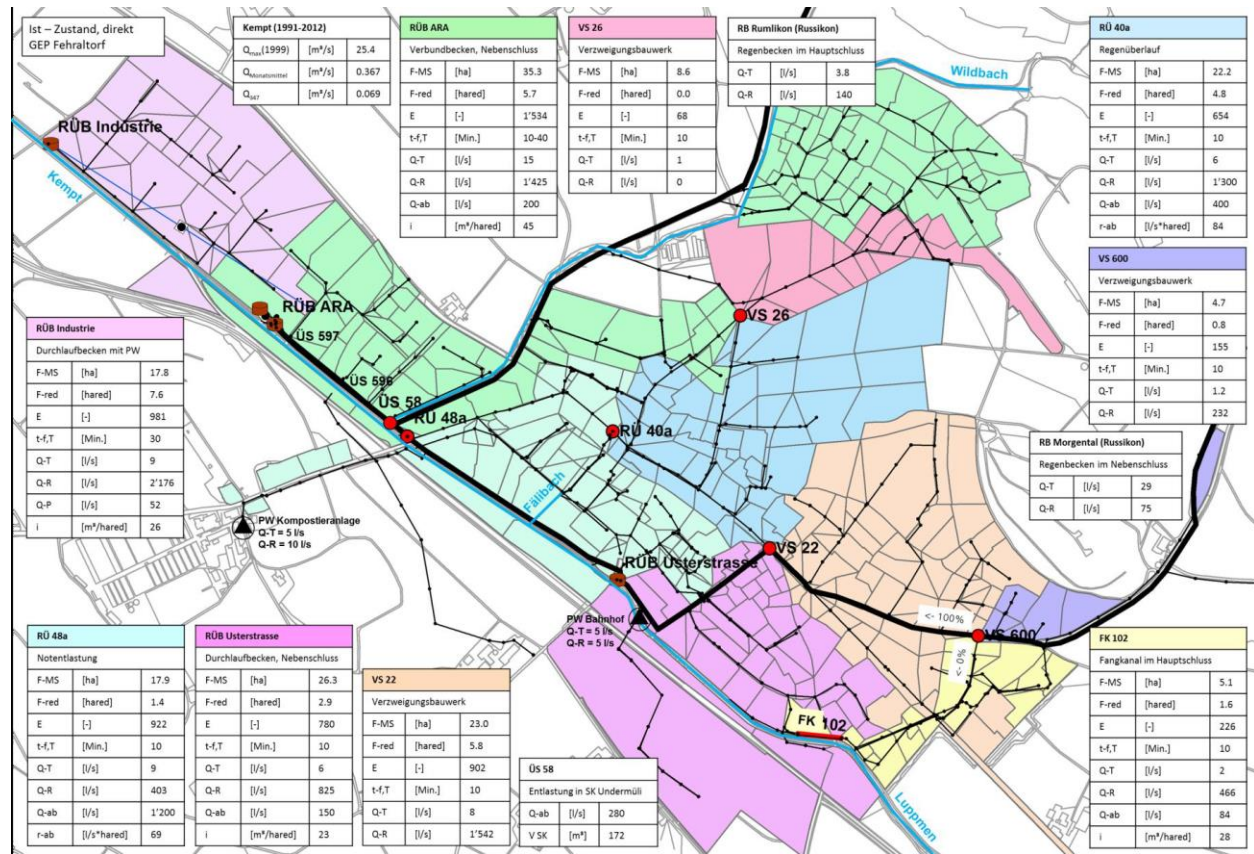


Figure S 7: Subcatchment characteristics for hydrological modelling. F-MS [ha]: total area of the combined system; F-red [ha] : Runoff-efficient area (combined sewer system); E_H :Inhabitants [-]; t-f,T [min]: flow time in the subcatchment ; Q-T [Ls⁻¹]: dry weather runoff (daily peak = daily mean * 2.4); Q-R [Ls⁻¹]: specific stormwater runoff for design storm; Q-ab [Ls⁻¹]: flow rate; i [m³ ha_{red}⁻¹]: specific storage volume; r-ab [Ls⁻¹*ha_{red}]: specific carry-on flow. (Figure corresponds to "Abbildung 10-4, Einleitschema im Ist-Zustand, Kennzahlen direkt" in HBT (2016))

⁷ VGEP - Generalentwässerungsplan des Abwasserverbands (in German). Urban Drainage Master Plan concerning the catchment area of the regional wastewater utility.

⁸ GEP - Generalentwässerungsplan (in German) - Urban Drainage Master Plan

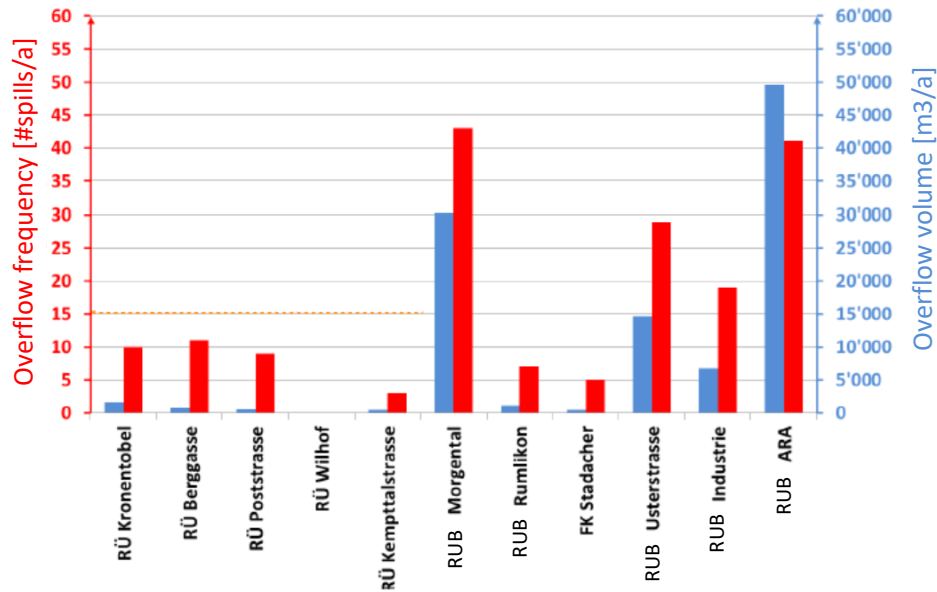


Figure S 8: CSO behaviour estimated within the scope of the General Urban Drainage Planning (HBT, 2016).

Overflow emissions: In 2012, combined sewer overflow (CSO) emissions were estimated using a hydrological model. Due to the lack of local long-term rain data, rain data from the MeteoSwiss rain gauge at Zurich-Kloten (airport) was used to drive the model. Although this particular rain gauge is located at a fair distance from Fehraltorf (ca. 14 km), the model's estimate was plausible, with an approximate variability of 10 % regarding the number of CSO spills for a period between 2008 and 2012. Main emissions originate from combined sewer overflows at RUB Morgenthal and RUB ARA/WWTP (cf. Figure S 8).

Rivers: Most combined sewer overflows discharge into small, sensitive streams, such as the Rohrbach, the Fällibach, and the Luppmen/Kempt. All watercourses eventually converge to form the river Kempt, which receives overflows from the final/most downstream overflow facility just upstream of the WWTP inflow and the continuous effluent discharge from the WWTP.

The influence of the WWTP on the River Kempt is small in terms of the pollutant load, but large with regard to hydraulic means (design flow capacity 170 L s^{-1}). During dry weather periods the hydraulic load introduced through the WWTP effluent (mean dry weather inflow: 38 L s^{-1}) may be in a similar range as the river baseflow. The monthly average discharge in the River Luppmen/Kempt at the WWTP is in the range of 367 L s^{-1} ; the statistical minimum discharge Q_{347} ⁹ is 69 L s^{-1} .

⁹ River discharge that is exceeded on 347 days of the year.

S2.2 Municipal water use, wastewater characteristics and sewer infiltration

The Urban Drainage Master Plan (HBT 2016) provides fundamental information on water use, wastewater characteristics, pollutant loads and sewer infiltration. This data has been derived from analysing the WWTP inflow rate data recorded during 2008 and 2012:

- Mean dry weather inflow: 38 L s^{-1} , mean value of all dry weather days
- Mean sewer infiltration rate (referred to total dry weather flow): 42 %
- Mean daily COD load: $1'454 \text{ kg COD d}^{-1}$
- Mean daily $\text{NH}_4\text{-N}$ load: 64.8 kg N d^{-1}
- Mean daily P_{tot} load: 19.1 kg P d^{-1}

On the basis of these analyses, the water consumption per inhabitant and the level of foul sewage pollution (COD load) were estimated to:

- mean daily water consumption $184 \text{ L cap}^{-1} \text{ d}^{-1}$
- foul sewage COD concentration 696 mg L^{-1}
- foul sewage $\text{NH}_4\text{-N}$ concentration 31.8 mg L^{-1}
- foul sewage P_{tot} concentration 8.8 mg L^{-1}

The maximum dry weather flow rate was measured to be 90 L s^{-1} . The hydraulic design capacity of the WWTP was assumed to be 170 L s^{-1} .

S3 Stormwater treatment and flow control structures

S3.1 Overview on hydraulic network structures

The following sections provide detailed information on most relevant hydraulic network structures in the Fehrlortorf-Russikon drainage system, including stormwater treatment facilities, in-sewer storage channels, flow splitters, pumping stations, and control structures. The drainage layout and topological relevance of these structures is illustrated in the hydrological flow scheme in Figure S 9. Table S1 summarises key information for the most relevant structures.

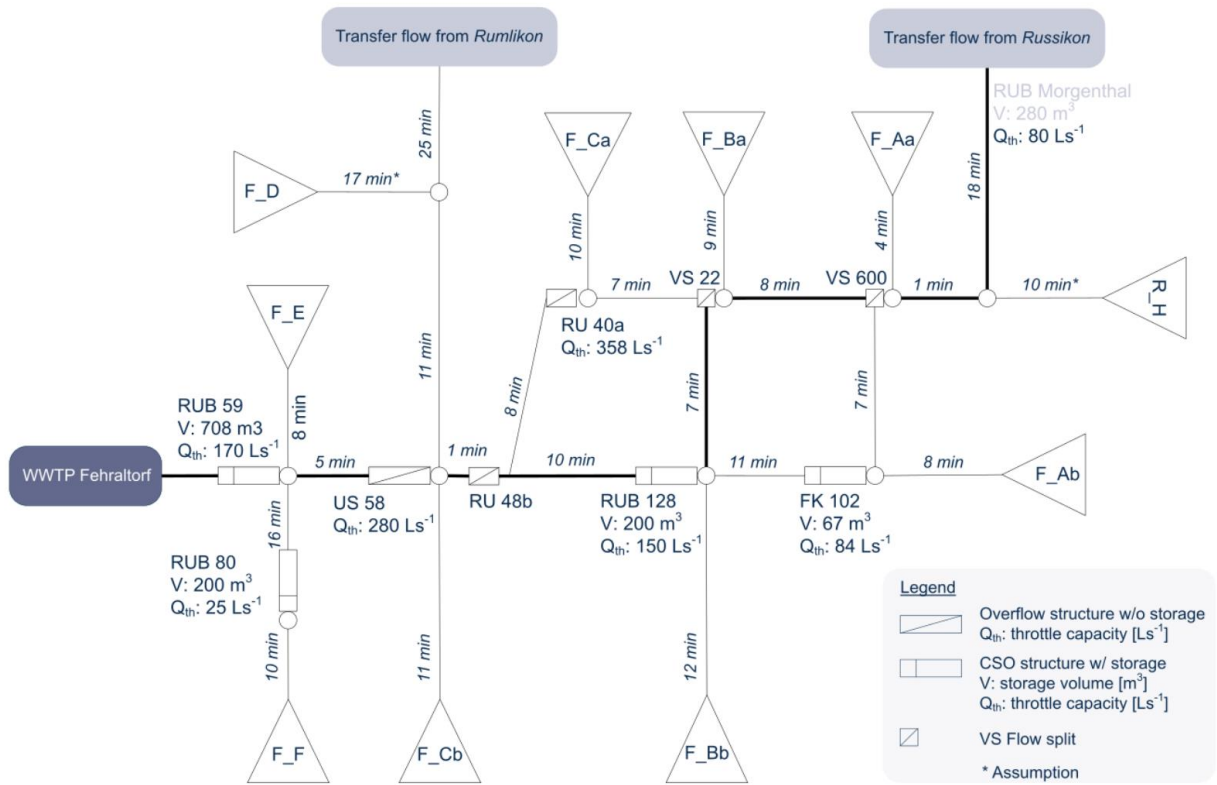


Figure S 9: Hydrologic flow scheme of the Fehrlortorf (combined) sewer network. The main flow path (bold line) is from top right (RUB Morgenthal) to the left (WWTP Fehrlortorf). Triangles represent aggregated sub-catchments. Indicated flow times are estimated assuming an average flow velocity in the sewer of $1 m s^{-1}$ and verified through field experiments. Cf. Figure 2, main paper. Version: 15-Jan-2024.

Table S1: major components in the sewer network of Fehraltorf-Russikon

Name	Alias name	Structure type	Retention volume [m ³]	Overflow to..	Routine monitoring?	Drainage relevance
RUB ¹⁰ Morgenthal	-	Catch basin operated in bypass mode	280 (+145)	Rohrbach	Yes, tank level	Stormwater treatment facility that concludes drainage system of Russikon; flow limiter: Vortex
FK ¹¹ 102	FK Stadacher	In-sewer pipe storage with upstream outlet (bar rake)	67	Luppmen/ Kempt	Yes, level sensor	Few registered overflows; utilisation heavily influenced by upstream flow splitter VS600
RUB 128	RUB Usterstrasse	Flow-through basin in bypass mode	200	Luppmen/ Kempt	Yes, tank level	Carry-on flow limiter: pipe throttle
RUB 59	RUB ARA ¹²	Flow-through basin in bypass mode	540 + 172	Luppmen/ Kempt	Yes, tank level	Largest overflow structure that concludes the drainage system Fehraltorf
RUB 80	RUB Industrie	Flow-through basin in bypass mode	200	Luppmen/ Kempt	Yes, tank level	Carry-on flow is pumped to eventually drain just upstream of the WWTP
RU ¹³ 40a	RU Kempptalstrasse	Stormwater overflow w/o retention volume	-	Fälibach -> Luppmen/ Kempt	No	
RU 48b		Stormwater overflow w/o retention volume	-	Luppmen/ Kempt	No	emergency overflow; the overflow structure is considered as inactive
VS ¹⁴ 600		In-sewer flow split	-	FK 102	No	
VS 22		In-sewer flow split	-	RU 40a	No	
US ¹⁵ 58	58_SBW	Controlled in-sewer overflow structure; slide gate	-	RUB 59	No	Flow control device that limits the WWTP inflow was changed in 08/2020

¹⁰ RUB: Regenüberlaufbecken (German) – stormwater overflow with retention volume, i.e. storage tank

¹¹ FK: Fangkanal, i.e. Stauraumkanal (German); in-sewer storage facility

¹² ARA: Abwasserreinigungsanlage (German) – wastewater treatment facility

¹³ RU: Regenüberlauf (German) – stormwater overflow without retention volume

¹⁴ VS: Verteilschacht (German) – in-sewer distribution chamber

¹⁵ US: Überlaufschacht (German) – in-sewer overflow chamber

S3.2 Stormwater treatment facility *RUB Morgenthal*

RUB Morgenthal plays a crucial role in the urban drainage system of *Fehrltorf*, although it formally belongs to the municipal drainage network of *Russikon*. This structure restricts permissible flows from the *Russikon* drainage system into the central *Fehrltorf* drainage system. The retention tank, with a total volume of 280 m³ (including the retention tank and inflow chamber), is equipped with a vortex-type flow limiter, limiting the maximum carry-on flow to the wastewater treatment plant (WWTP) to 75 L/s (Q_{th}). The spillway, featuring a nominal pipe size of 1,000 mm, discharges into the Rohrbach creek. For better illustration, the longitudinal cross-section and a 3-D layout is given in Figure S 10.

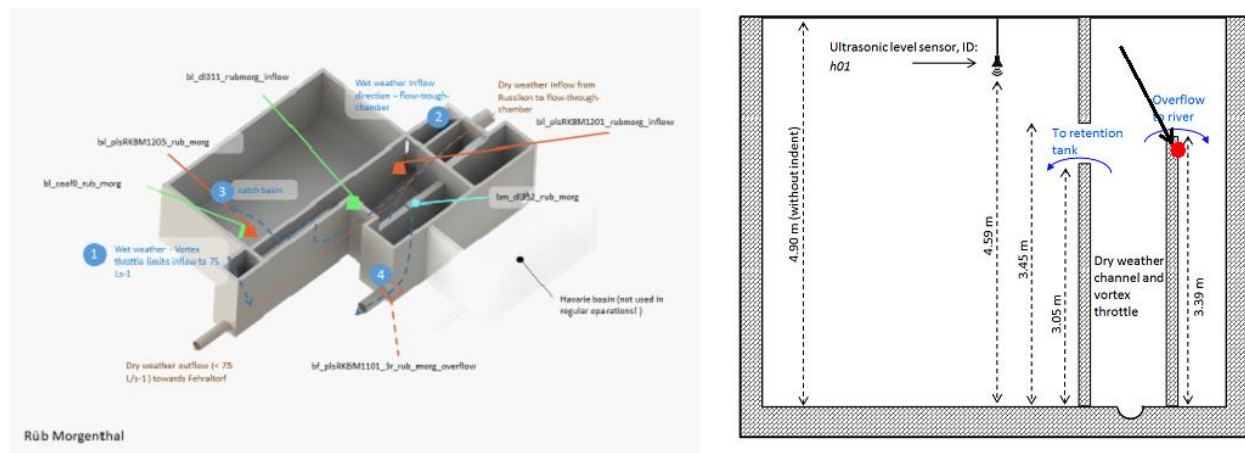


Figure S 10, left: 3-D drawing of the *RUB Morgenthal*, including sensor positioning and flow path during wet weather. Right figure: Cross-section through the overflow structure *RUB Morgenthal* (not drawn to scale) including inflow chamber, retention tank, overflow to receiving water and installed sensors.

Hydraulic functioning: in case the inflow exceeds Q_{th} , wastewater backs up within the flow-through chamber (cf. Figure S 10, left, from 1 to 2) until it reaches a water level of 3.05 m above invert of the retention tank. If the water level exceeds 3.05 m, excess water overflows into the retention tank (catch basin; 3) until it reaches a filling level of about 3.39 m. At this point, an overflow takes place (4). The catch basin is emptied by gravity, i.e. through a valve that opens as soon as the throttle discharge rate has decreased to nearly dry weather conditions, i.e. below a threshold of 30 L s^{-1} . The retention tank is cleaned on demand through a flushing bucket system. In case of emergency, e.g., wastewater contains specifically water-endangering substances, polluted wastewater can be retained in a separate basin. The structure was built in 1963 as “emergency basin”. It provides an additional storage volume of 145 m³; however, the emergency basin is not put in operation for typical stormwater management.

S3.3 In-sewer storage facility FK 102 (FK Stadacher)

The in-sewer storage with an overflow weir at the upstream end (FK 102 – Stadacher) runs parallel to the Luppmen for about 100 m and has a storage volume of 67 m³ (Figure S 11). The carry-on flow of the in-sewer-storage is limited to a range of 35 - 40 L s⁻¹ by a vortex flow limiter. A bar rake additionally filters solids before the overflow into the watercourse on the overflow weir with a crest length of 6 m. The storage channel is emptied automatically after the inflow has been reduced. The relevance of the structure in the overall hydraulic context is low. Due to the high overflow / weir crest level at the flow splitter 600 (VS600) and the additional vortex throttle at RUB Morgenthal (limited to 75 L s⁻¹) upstream, an overflow occurs only during extreme events.

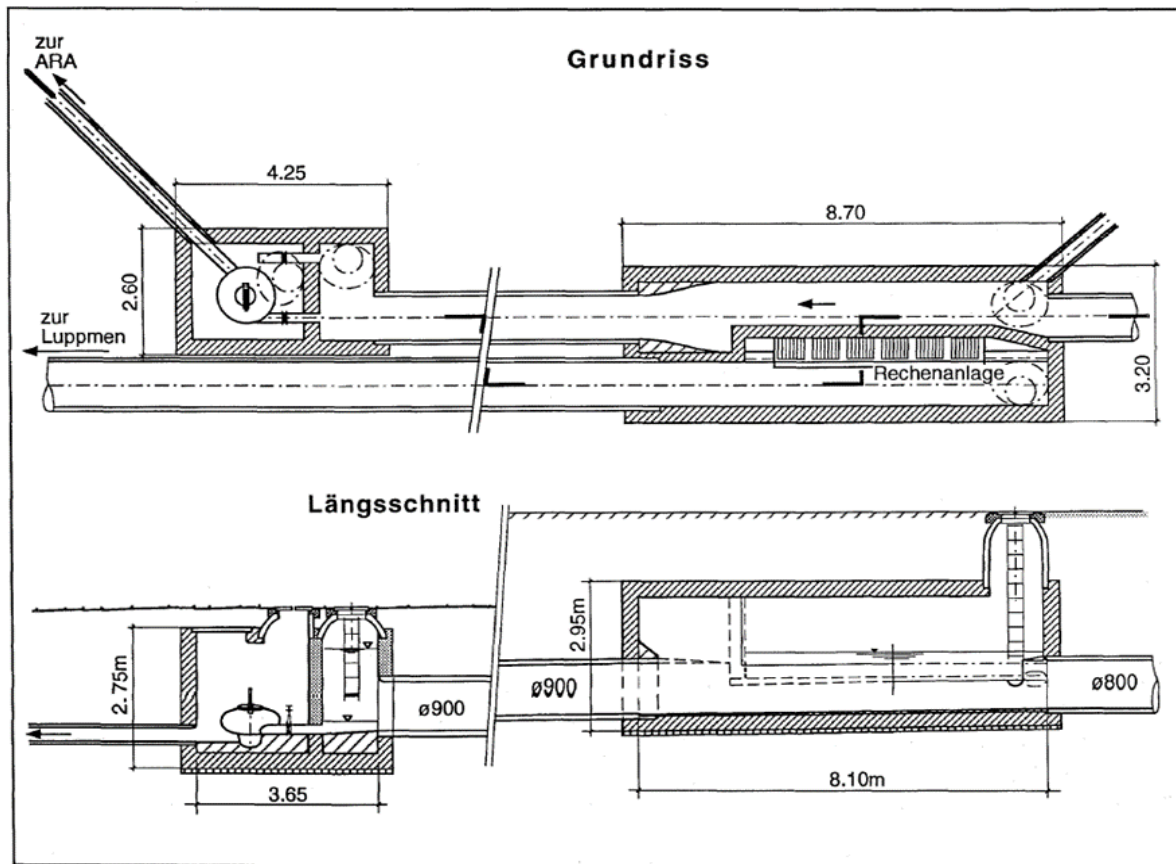
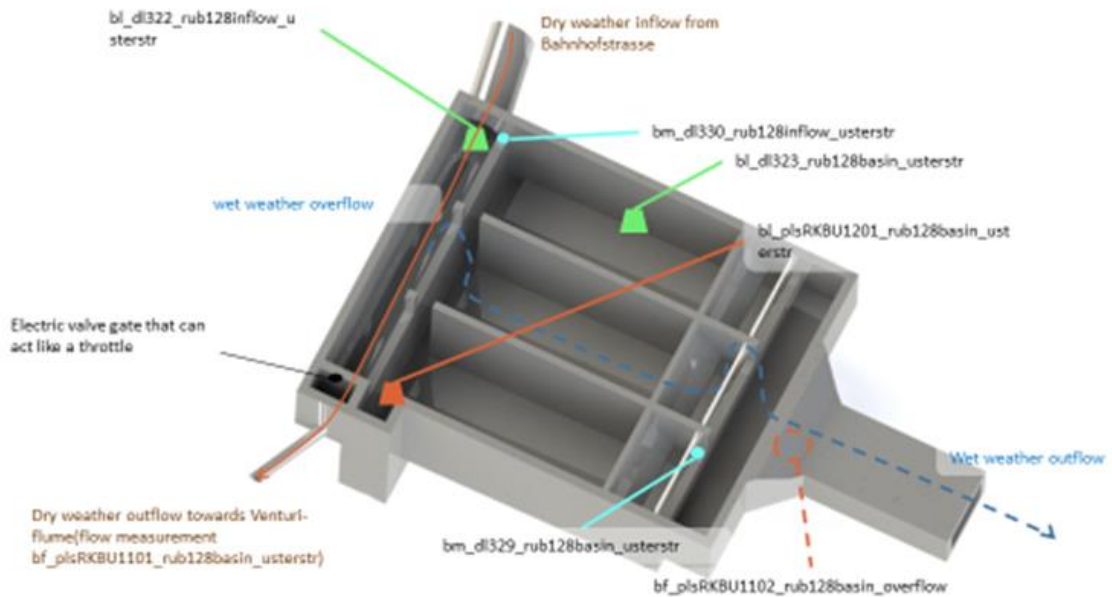


Figure S 11: Top: FK 102 - planar view (Grundriss); bottom: FK 102 - longitudinal cross-section ("Längsschnitt") - taken from Krejci (1994).

S3.4 Stormwater treatment facility *RUB 128 (RUB Usterstrasse)*

The offline CSO tank (Becken im "Nebenschluss") has a storage volume of 200 m³ (Figure S 12). The carry-on flow is limited by a static pipe throttle (nominal reduction from DN 1250 mm to DN 400 mm) to approx. 150 L s⁻¹. In addition, the flow can be further limited by means of an electric-hydraulic gate valve, which is however currently not active in daily operation. Just downstream of the pipe throttle, there is a Venturi flume, that allows for permanent flow monitoring. In case of rainfall, the basin fills up and discharges via three transversal overflow weirs - each section is 3 m wide - into the buffer chamber and from there further into the *Luppmen*. The basin is emptied with a submersible sewage pump. After emptying, the basin is cleaned through an automatic flushing bucket system.



Rüb 128 Usterstr

Figure S 12: 3-D drawing of the *RUB 128*, i.e. *RUB Usterstrasse* including sensor positioning and flow path during wet weather (blue, dotted line).

S3.5 Stormwater treatment facility *RUB 59 (RUB ARA)*

The RUB ARA (Figure S 13) is the largest stormwater treatment facility in the Fehrlortorf system, hydrologically the network-concluding overflow structure just upstream of the WWTP. It is operated as flow-through basin in bypass mode. It has a tank storage volume of 540 m³; another 172 m³ of in-sewer storage volume can be activated in the upstream backwater channel.

Until 2020, the inflow to the wastewater treatment plant (WWTP) was monitored using a level sensor and controlled to a calculated maximum inflow of 180 L s⁻¹ through an electric-hydraulic slide gate at the in-sewer flow splitting structure US 58. In August 2020, a flow control system from Stebatec AG (type TF-PNA¹⁶) was implemented at the sewage treatment plant inlet. The operation mode of the RUB ARA remains unchanged, except that the impoundment point is closer to the WWTP. Thus, the upstream storage volume has increased. In addition, the inflow measurement has become more precise.

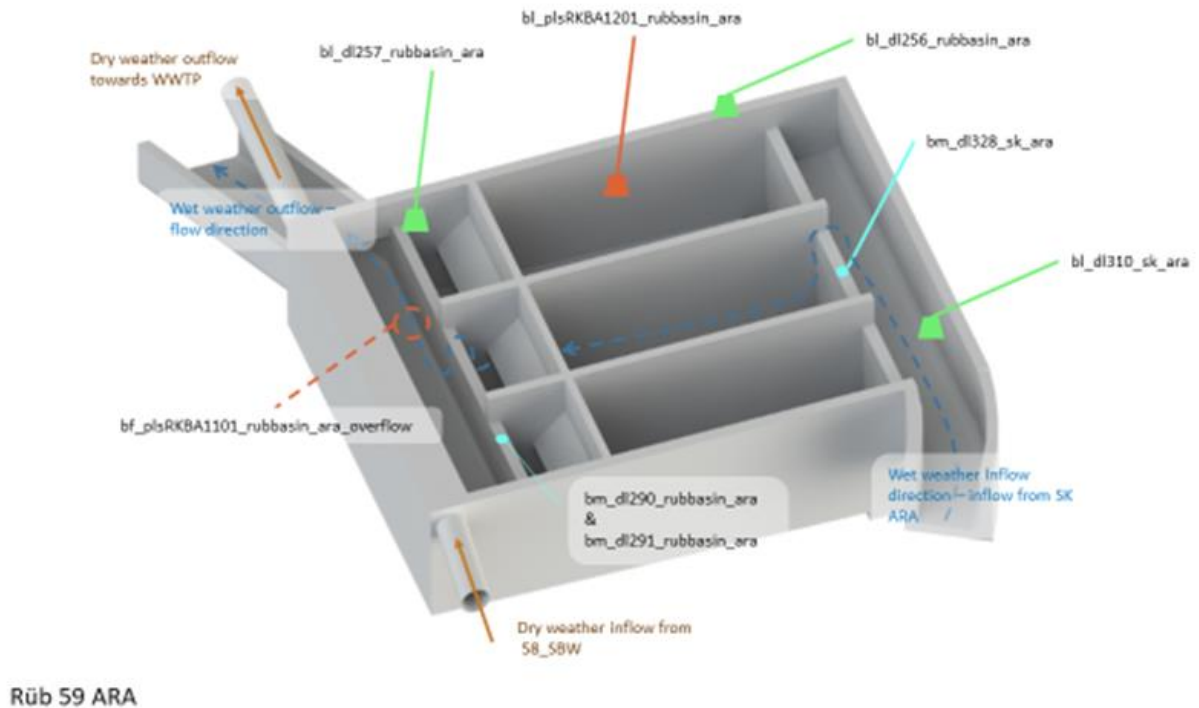
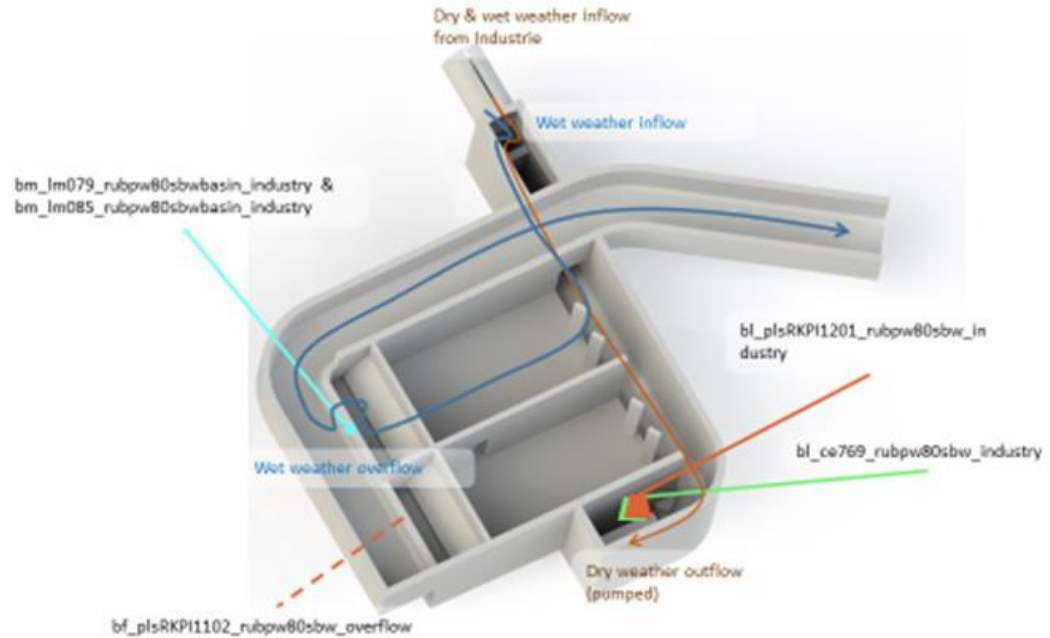


Figure S 13: 3-D drawing of *RUB 59*, i.e. *RUB ARA*, including sensor positioning and flow path during wet weather (dotted blue line).

¹⁶ Teilgefüllte pneumatische Pneumatische Abflussregelung (TF-PNA)- Pneumatic discharge control, partially filled

S3.6 RUB PW80 (RUB Industrie)

The flow-through basin with pumping station RB80 Industrie (Figure S 14) has a basin volume of 200 m³. During dry weather, the wastewater is lifted by two pumps and then conveyed to the wastewater treatment plant through a gravity pipe. In case of rainfall, the overflowing wastewater is discharged into the Kempt. The tank emptying is coupled with the pumps from the dry weather outflow. The basin is cleaned on demand by a flushing-bucket system.



Rüb Industrie

Figure S 14: 3-D drawing of RUB PW80 (RUB Industrie), including sensor positioning and flow path during wet weather.

S3.7 Flow splitting structure VS600

The flow splitter VS600 (Figure S 15) is located 300 m downstream of the RUB Morgenthal in the main collector, conveying dry weather flows into the direction Russikerstrasse. In case of heavy rainfall and elevated water levels, an in-sewer side overflow allows wastewater to flow into a secondary collector (Feldstrasse) eventually leading to the in-sewer storage facility *FK 102*. With limiting the flow at RUB Morgenthal to a maximum of 75 L s^{-1} (no significant contributions in between, i.e. downstream of RUB Morgenthal), during almost 100 % of the time the flows travel into the direction of Russikerstrasse. Side overflows towards the collector at *Feldstrasse* are only observed in very few cases.



Figure S 15: Flow splitter VS600 with slide gates (photo taken from the GEP – HBT, 2016).

S3.8 Flow splitting structure VS 22

The flow splitter VS 22 (Figure S 16) is operated manually and for maintenance purposes only. The slide gate remains nearly fully open, the flow follows the main flow path to *RUB 128*. An overflow, i.e. diversion via the transversal weir structure further to the in-sewer overflow structure *RU 40a (RU Kempttalstrasse)* practically never happens during wet weather conditions. Wet weather flow dynamics are dampened since the carry-on flow from the RUB Morgenthal is per se limited and flow contributions in between are minor.



Figure S 16: Flow splitter VS22 with a manually operated gate at the outlet. The arrow indicates the possibility of in-sewer overflows diverting the sewage to *RU 40a* (photo taken from HBT 2016).

S3.9 Flow control structure *RU 40a*

The in-sewer stormwater overflow *RU 40a* (Figure S 17) is a relief system into the Fälibach/Luppmen. The facility includes a slide gate to control the outflow. The slide gate at the flow distribution structure *VS22* just upstream can be used to control the inflow. As the open flow gate in the upstream structure *VS22* never opens, overflows can only occur during very extreme rain events.



Figure S 17: Overflow chamber *RU 40a* with slide gates (photos taken from HBT, 2016; modified). The left and right pictures show a downstream and upstream view. The numbers 1 and 2 label same points of reference and the arrow indicates downstream flow direction.

S3.10 In-sewer flow distribution facility *US 58*

A few hundred meters upstream of the WWTP inlet structure, the flow in the main collector can be split, i.e. diverted into an in-sewer storage channel (total volume: 172 m³) that eventually leads to the central RUB 59 (total volume: 540 m³) (Figure S 18). Until July 2020, a slide gate actuator served as the primary control element to limit flow to the WWTP during wet weather periods. It was also used for maintenance purposes. Since August 2020, a pneumatic, partially-filled flow control device (Fa. Stebatec, Brugg CH) has been installed to control the inflow of the WWTP. Since then, the main collector just upstream of the WWTP inlet has also been used temporarily as additional in-sewer storage. This “operational storage” is not accounted for in the volume mentioned above.



Figure S 18: In-sewer flow diversion structure *US 58*. Until mid-2020, the penstock actuator served as the primary control element to limit the inflow to the WWTP. The bottom channel (left picture) is the main dry weather inflow towards the WWTP. Middle picture: broad-crested overflow weir and inlet into the in-sewer storage channel that runs in parallel towards the *RUB 59 (RUB ARA)*.

S3.11 Stormwater overflow *RU 48b* (emergency overflow)

The stormwater overflow *RU 48b* is currently not in operation (Figure S 19). It is assumed that overflows from the main collector into the Luppmen creek are very unlikely to occur. On the other hand, backwater intrusion into the urban drainage system due to river flooding in the nearby Luppmen creek may occur. The WWTP personnel has reported the presence of driftwood in WWTP inlet structures after extreme rainfall or flood events. The overflow structure is hydraulically not relevant, but it is named here for the sake of completeness.



Figure S 19: Stormwater overflow *RU 48b*, which is considered inactive under given circumstances.

S4 Sensor classes

S4.1 Rain gauge: *RM Young 52202*

The RM-Young tipping bucket rain gauge¹⁷ (Figure S 20) is a widely used factory calibrated sensor that is connected to a DecentLab LoRaWAN-logger¹⁸. It fulfills also the WMO-guideline No. 8 as a quality standard. Internal wake-up's of the Decentlab-Logger count each tip and sends the calculated rainfall_intensity and linked parameters over LoRaWAN further towards the Data pipeline. The circular collector funnel has a diameter of 18.5 cm resulting in a catchment area of 200 cm². Its measurement resolution is 0.1 mm per tip. Due to the low-power consumption and data transmission the unheated version of the sensor was used. This leads to not reliable data in winter times.

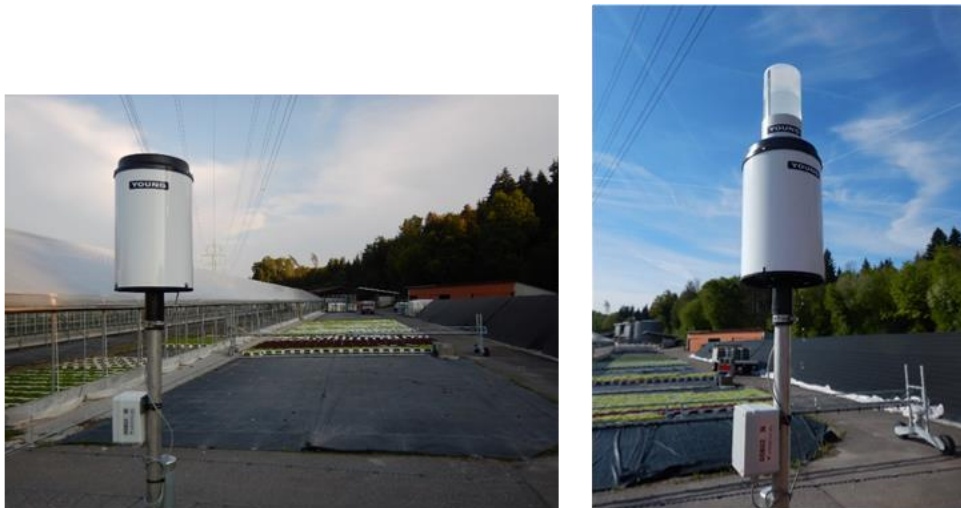


Figure S 20: RM young with LoRaWAN-logger attached to the stand pole; right: rain gauge calibrator in action

Maintenance has been performed in irregular time intervals about every 10 months. This consisted in checking the total number of tips for a predefined volume (Gauge Calibrator¹⁹, RM Young). The rainfall intensity could only be checked approximated due the insufficient temporal resolution of the 5 min transmission interval. Further visual inspection of the mechanical stand and spirit leveling as well as the cleaning of tips and the entry funnel from debris have been performed.

Relevant Parameters in the dataset are “rainfall_intensity” and “rainfall_cumsum”. The rainfall_intensity is the main measurement value. With regard of the package loss in the data transmission the rainfall_cumsum (cumulative sum from the logger) is the second important variable in the dataset. During operation several clogging-events of the entry funnel happened and errors occurred. The “operators convenience flag” in the metadata provides the information from the suggested clogging start until end time (terminated by maintenance).

¹⁷ <https://www.youngusa.com/product/tipping-bucket-rain-gauge/> (data access 20.07.2023)

¹⁸ <https://www.decentlab.com/products/tipping-bucket-rain-gauge-for-lorawan> (data access 20.07.2023)

¹⁹ <https://www.youngusa.com/product/rain-gauge-calibrator/> (data access 20.07.2023)

S4.2 Rain gauge: *Ott Pluvio 2L*

The Ott Pluvio 2L²⁰ (Figure S 21) is an accurate weighing rain gauge that has a reputation to provide reliable rain data with very little no maintenance and fulfills WMO guideline No.8. It uses a high-precision load cell and internal algorithms to compensate several factors to produce really good results. The catchment area is 400 cm² and the unheated version has been used in the UWO. Pallets have been used, with a heavy concrete base for levelling. The data is sent via the mobile phone network. The power supply is self-sufficient via a solar panel with battery.

The most important parameter measured is "rainfall_intensity". It corresponds to the combined (realtime RT/ non realtime(NRT) – value that is provided by the rain gauge itself. The parameter "accumulated total rainfall" indicates the amount of precipitation since the last reset or battery change. A reset on a regular basis haven't been performed. Twice a year a visual inspection and cleaning (spirit leveling, animal nests) as well as an bucket emptying have been performed. Further a weight accuracy test has been performed once a year and in autumn a glycol-water solvent filled up to prevent damage through ice.



Figure S 21: Two examples of stand-alone rain gauge locations in the UWO

²⁰ <https://www.ott.com/en-uk/products/meteorological-sensors-101/ott-pluvio2-l-weighing-rain-gauge-2374/> (data access 20.07.2023)

S4.3 Water level: *Maxbotix MB 7389/7369*

The Maxbotix is a weather-resistant rugged ultrasonic sensor component module with IP68 rating (Figure S 22). It is an advanced sensor, which is designed to report the distance to the largest acoustic target while ignoring smaller return signals. Series MB 7389 and MB 7369²¹ only differ in the connector interface (TTL / RS232) and will be described as the same sensor for simplicity. The sensor can measure in a range of 300-5000 mm with a very low power design that makes it suitable for long-term battery operation. It has an internal temperature compensation. The sensor uses the “Most Likely Filter”²² to return the largest target as seen from the sensor and ignore smaller ultrasonic echoes. The sensor is either connected to the first own produced prototypes or to a Logger from Decentlab²³. Both are sending the data over LoRaWAN. In most monitoring sites, the logger has been placed close to the manhole cover and the sensor close to the wastewater to obtain both the best sensor performance and the best data transmission.

Maintenance has been done on an irregular schedule on demand. Visual inspections, especially for perpendicular sensor alignment to the flow, reference level measurements and mechanical cleanings have been performed. The most important measurement values are the water_level which is converted in the datapool application. Further the “Trials”-value gives an indicator on the measurement quality (0-15 ; 15 means 15 measured same values after another). For the first prototypes this parameter only exists internally (or a median of 15 values has been computed).



Figure S 22: Example installation of the rugged water level sensor Maxbotix sensor in the sewer. The cable makes it possible to place the sensor in a different spot at the monitoring site than the logger. This is important to optimize both sensor performance and data transmission.

²¹ <https://maxbotix.com/products/mb7389> (data access 20.07.2023)

²² <https://maxbotix.com/pages/hrxl-maxsonar-wr-datasheet> (data access 20.07.2023)

²³ <https://www.decentlab.com/products/ultrasonic-distance-/-level-sensor-for-lorawan> (data access 20.07.2023)

S4.4 Capacitive overflow detection: *Meter 5TM*



Figure S 23: Left: the Decagon sensor, i.e. Meter 5TM mounted on a weir crest in dry environment; right: submerged sensor in case of an overflow event.

The Decagon, i.e. Meter 5TM²⁴ is a soil moisture sensor that also measures temperature (Figure S 23). The sensor is “re-used” as a binary, low-cost overflow detector on weir crests since a substantial shift can be detected in the observations of volumetric water content when the sensor is submerged in overflowing stormwater. Usually a sensor got mounted at the inflow into the basin as well as at the overflow to give further information about the overflow activity (0/1; overflow duration).

The measurement method is capacitive and thanks to the SDI-12 protocol the sensor is low power. The logger (Decentlab) transmits the data via LoRaWAN.

Main measurement parameters are `dielectric_permittivity` and `overflow_temperature` in the dataset. The values of the dielectric permittivity have not been converted to a binary signal in the given UWO dataset.

²⁴ <https://metergroup.de/environment/produkte/5tm-volumetrische-feuchte/> (data access 20.07.2023)

S4.5 Temperature: *dual temperature sensors*

For a specific use case for temperature in the sewer, DS18B20 digital sensors²⁵ (Figure S 24) were used to measure a) the air temperature at the sewer crown and b) the water temperature. The sensor itself offers the advantage of measuring the temperature cost-effectively and already digitised in the sensor head which makes it easy for the signal processing. For the air temperature, an additional weather protection housing was manufactured using additive manufacturing (Material Extrusion MEX). The water temperature sensor was mounted flexibly, with an additional protective hose and weight ensuring that the sensor remains in the water but can also be deflected. Both sensors were connected to a Decentlab-Logger²⁶.



Figure S 24: Example installation of a dual temperature sensor, which simultaneously record temperatures of the wastewater and the sewer atmosphere.

For this sensor no specific maintenance protocol has been implemented. Where some sensors were present in the same location, a visual check and manual cleaning was carried out, but in most cases this was not recorded in the metadata. Most relevant parameters are “headspace_temperature” and “water_temperature” in the dataset.

²⁵ <https://www.stg-maximintegrated.com/en/products/sensors/DS18B20.html> (data access 20.07.2023)

²⁶ <https://www.decentlab.com/products/temperature-sensor-for-lorawan> (data access 20.07.2023)

S4.6 Flow and velocity: *Flo-Dar, Marsh-MCBirney*

The Flo-Dar AV²⁷ sensor (Figure S 25) provides a non-contact, intrinsically safe and portable flow monitoring. It uses digital Doppler Radar technology for the measurement of the surface velocity as well as an ultrasonic pulse echo water level measurement. The conversion and logging is done with an FL900 series logger where an obsolete 2G-logger sent the data over mobile phone network. The Flo-Dar provides very good results especially in smaller channels with low-flow or fast discharge.

The most relevant parameter in the dataset is the “flow_rate” as well as the calculated “average_velocity” and “water_level”. For in-depth analysis for the measurement quality the quality value “pmr” and “nos” can provide further information. Maintenance has been done on an irregular basis 1-2x per year (device cleaning, visual check alignment, reference measurement). Only the water_level had been adjusted over time from the reference-measurement since the “truth”-value for the velocity just has been compared to a portable flow meter²⁸.



Figure S 25: Flo-Dar installed in manhole during comparison with portable flow meter

²⁷ <https://www.hach.com/p-flo-dar-av-sensor-with-optional-surge-velocity-sensor/MODEL%204000-900> (data access 20.07.2023)

²⁸ <https://www.otthydromet.com/en/p-ott-mf-pro-portable-flow-meter/1040500595-0D> (data access 20.07.2023)

S4.7 Flow and velocity: Sommer SQ-3

The Sommer SQ-3 flow meter (Figure S 26) is measuring velocity with a Doppler-radar at 24 Ghz and an ultrasonic level measurement. A newer version of the sensor(SQ-R ; not used in the UWO) uses other Doppler-radar frequencies as well as radar level measurement where documentation can be found online²⁹. It has an automatic vertical angle compensation and offers very good measurement results in low-flow or fast flow conditions. With the connected MRL-7 logger the data gets transmitted over cellular network by 3G.

The most important parameters for the dataset are “flow_rate” as well as the related “water_level” and “surface_velocity”. The “snr”, “gain”, “bandwidthclass” can provide in depth analysis parameter for further understanding. unfortunately, just the surface_velocity or the calculated_velocity can be tracked. Maintenance has been done similar to the Flo-Dar on an irregular basis 1-2x per year (device cleaning, visual check alignment, reference measurement). Only the water_level had been adjusted over time from the reference-measurement since the “ground truth”-value for the velocity just has been compared to a portable flow meter.



Figure S 26: Sommer SQ-3 flow meter in a “low-flow” measurement site.

²⁹ <https://www.sommer.at/en/products/sewage-wastewater/sq-flow-meters> (data access 20.07.2023)

S4.8 Flow and velocity: *NIVUS POA/CSM sensor*

NIVUS correlation wedge sensors³⁰ (Figure S 27) delivers flow measurements with a mobile system and ATEX certificates. In comparison with the radar technology the velocity over height gets measured in reality. The correlation wedge sensor need a minimum of fill level to operate properly and not too fast discharge. The data gets logged at the PCM Pro Ex and transmitted over a cellular network in 2G.

Maintenance has been done on a regular basis twice a year (cleaning of in-situ-sensor with a rod brush, reference measurements and so on). Further some cleaning and checks with system removal have been done when the data quality was unsatisfying (e.g. debris on sensor that flow went to 0 Ls⁻¹). The parameter “flow_rate” is the most important parameter together with the related “average_velocity” and “water_level”. Additionally, the parameter “water_temperature” gets also measured.



Figure S 27: Nivus POA correlation wedge sensor(barely seen on the ground) inside the sewer

³⁰<https://www.nivus.com/en/products-solutions/measurement-systems/flow-measurement-for-liquids/flow-meters-part-filled/flow-sensors/poa-correlation-wedge-sensor> (data access 20.07.2023)

S4.9 Weather and climate: *SHT-21/35*

The Sensirion SHT-21 or 35 is a temperature and humidity measurement sensor (Figure S 28) known for its ability to provide relatively accurate measurements when equipped with a radiation shield (passive ventilation). However, it is important to acknowledge that the passive ventilation introduces a certain level of error. The sensor signal is recorded with a Decentlab-logger which transmits the data over LoRaWAN³¹.

There has been no maintenance done on the sensors. Main measurement parameters are “ambient_air_temperature” and “relative_humidity”.



Figure S 28: Ambient temperature and humidity sensor mounted at a lamp pole (backside).

³¹ <https://www.decentlab.com/products/air-temperature-and-humidity-sensor-with-radiation-shield-for-lorawan> (data access 20.07.2023)

S4.10 Water level: *Keller 36KyX*

Pressure probes from Keller Druck (Figure S 29) offers good measurements of the water level³². The sensors were initially bought for sewage application but were used finally in the creeks to observe relative changes in water level. Pressure probes are excellent for low-power-applications and the data was collected and sent by a DecentLab-Logger³³.

Maintenance have been barely on an irregular basis with reference measurements and calibration, sensor cleanings and installation changes. The parameter “water_level” represents only relative changes in the creek and not absolute.



Figure S 29: Pressure probe inside a protective hull connected with the LoRaWAN-logger

³² <https://keller-druck.com/en/products/level-probes/standard-level-probes/series-36kyx> (data access 20.07.2023)

³³ <https://www.decentlab.com/products/pressure-/liquid-level-and-temperature-sensor-for-lorawan> (data access 20.07.2023)

S4.11 Data transmission: *LoRa-based mesh system*

LoRa-based mesh logger systems (Figure S 30) represents a logger platform that has been developed in a research project together with the ZHAW Winterthur³⁴. It offers the possibility to measure data in the underground and transmit it to a overground repeater station with LoRa protocol. The repeater station can collect data from multiple underground nodes. The repeater sends then the data further over LoRaWAN protocol to the standard gateways. The connected sensors were Maxbotix and Decagon-Series. In the source_id the LoRa-Mesh nodes can be identified by containing “lm” in the id.



Figure S 30: LoRa-Mesh repeater node (upper box) self-sufficient with the Solar Panel

³⁴ For further details it is referred to Ebi et al., 2019 (<https://ieeexplore.ieee.org/document/8703036>)

S4.12 Utility routine monitoring - PLS data

The Fehrltorf Water and Wastewater utility uses a number of different devices to routinely monitor flows and water levels at several locations (Fa. Nivus, Vega, Stebatec). The so collected data are archived in the utility's process control system (PLS). Due to the fact that only the actual measurement values are recorded, i.e. meta-data on sensor changes and maintenance do not exist, PLS data are assumed to be correct and non-erroneous. A major change however is that the WWTP inflow measurement system changed from an erroneous "water-level-to-flow-estimation" to a pneumatic, partially-fill flow control and measurement system (TF-PNA, Stebatec, Brugg³⁵) (Figure S 31). This system provides more reliable information on WWTP inflow since August 2020.



Figure S 31: Pneumatic flow limiter, partially-filled, at the main collector just upstream of the WWTP inlet.

³⁵ <https://www.stebatec.com/en/offers/pneumatic-flow-control-partially-filled-tfpna/> (data access 20.07.2023)

S4.13 Weather monitoring station *Lufft WS-700*

The compact weather station Lufft WS-700 (Figure S 32) offers high-quality monitoring all-in-one to observe microclimate³⁶. Though, the absolute accuracy of the rainfall intensity may be low due the radar measurement technology. But it delivers other important parameters like wind, ventilated temperature and humidity as well as global radiation and rainfall type. There has been no maintenance done on a regular basis. Monitored variables are:

- "ambient_air_temperature" (ventilated),
- "relative_humidity" (ventilated),
- "absolute_air_pressure",
- "relative_air_pressure",
- "wind_speed",
- "wind_direction",
- "rainfall_intensity" (use with caution),
- "global_radiation",
- "precipitation_type".

The "precipitation_type" can be a useful variable to identify if precipitation has been snow or rain.



Figure S 32: WS-700 on post with concrete base.

³⁶ <https://www.lufft.com/de-de/produkte/intelligente-wettersensoren-309/ws700-umb-intelligente-wettersensorik-2269/>
(data access 20.07.2023)

S4.14 Other sensors

There are a few “special” source types in the dataset, which were used for specific purposes. These are:

- 1x Davis Rain Gauge: (used to see how the performance is besides RM Young and an Ott Pluvio²L at Rub Morgenthal.
- 1x Decagon 10 HS & 1x Decagon ECTM: same as Decagon 5TM, slightly different models but used for the same purpose as described in Decagon (Meter) 5TM.
- 1x UIT GmbH TSIC: Temperature measurement chain from UIT GmbH, Germany. The measuring interval was set to 15 min. The sensor chain was deployed near a water distribution (DW) pipe as well as a wastewater (WW) pipe, buried in the ground (cf. 0) (Figure S 33). More details can be found in Boebel et al., 2023.

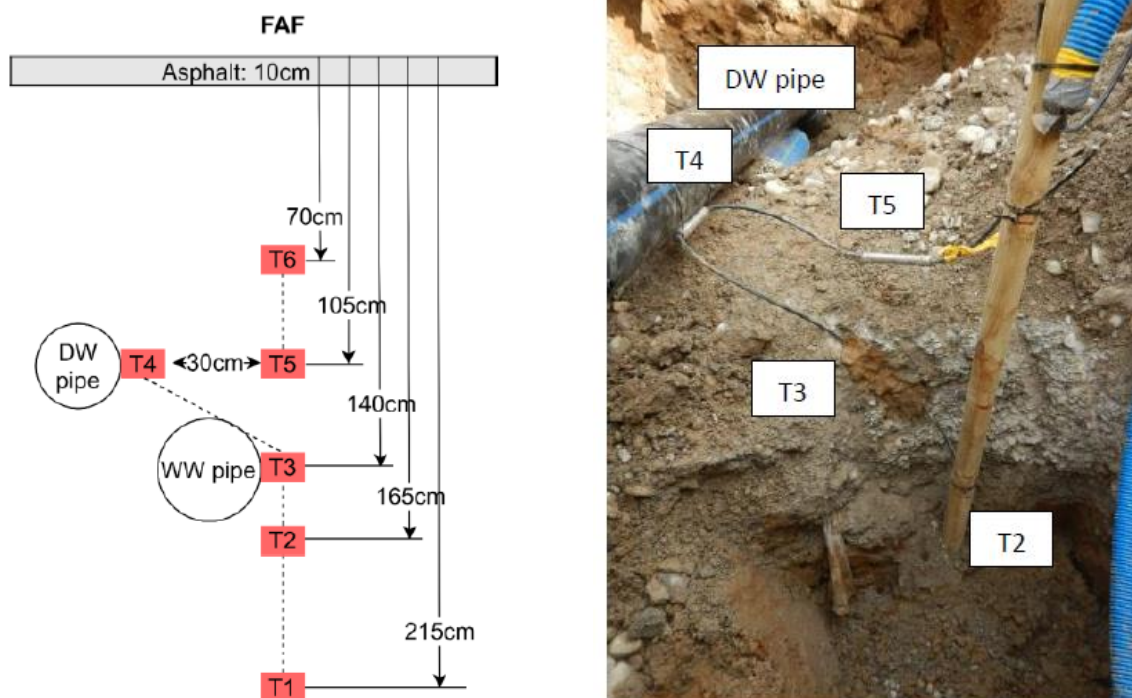


Figure S 33: left: principal draft of the temperature measurement positions ; right: photo at installation before they got buried in the soil.

Another small portion of the dataset contains information that is more or less irrelevant and remains as artifacts. Special attention should be given to the following source IDs before utilizing the data:

Source_id	Source_type	Notes
bt_dl4184_15a_russikerstr	SHT-35	Attempt to measure headspace temperature and humidity inside the sewer . Relative humidity observed was >100% most of the time
bx_ce792_450a_usterstr	DLN70	The CTD-probe was used to measure water level in a stormwater manhole for the municipality. Besides the level the probe measured conductivity & temperature.

S4.15 Gateways

In total 3 Gateways have been installed in Fehrlortorf to receive the LoRaWAN-data (Figure S 34 and Figure S 35). It was necessary to install multiple gateways to make sure most of the data gets transmitted from the underground. It remains very challenging to transmit data from underground structures with LPWAN protocols. The gateways were installed on high buildings spread over Fehrlortorf to cover most of the sensor location. For those locations where insufficient Quality of service occurred LoRa-based-Mesh was used to overcome the bottlenecks in transmission. Primarily Kerlink Wirnet iStations³⁷ have been used. One got replaced by a Tektelic Kona Macro IoT Gateway³⁸. Maintenance has been done on demand when an outfall of an area was observed and the error was found in the gateway.



Figure S 34: Gateway at the rooftop of a high rise building, including solar panels powering the entire system.



Figure S 35: Gateway at the rooftop of the Fehrlortorf WWTP control building.

³⁷ <https://www.kerlink.com/product/wirnet-istation/> (data access 20.07.2023)

³⁸ <https://tektelic.com/products/gateways/kona-macro-iot-gateway/> (data access 20.07.2023)

S5 Data storage and management in the “Datapool” warehouse

S5.1 The “Datapool” data warehouse

The “Datapool”³⁹ is an in-house data warehouse development of Eawag and ETH Zurich, SIS enabling structured sensor data management. The storage capabilities of the *Datapool* include the ability to handle different types of data such as time series, metadata, signal quality information, binary data, raster data and laboratory data in a *PostgreSQL* database with the PostGIS and TimescaleDB plugins. In the following we provide supporting information on the naming conventions and the data model. Further details can be found in the online documentation³⁷. How we track issues in the UWO dataset using a version control system is described in Section S5.6.

S5.2 General definitions used in the Datapool

Signal: A signal represents a measurement. Each signal represents a value of a measured variable at a given time and location.

Variable: The variable defines the measured quantity by specifying a name and a unit.

Source: A (data-)source is a specific measuring equipment. Every measurement (signal) originates from a specific source. The name of a source is unique.

Source-type: Sources with the same properties can be assigned to a source-type.

Site: A site represents the location where the measurement is taken. Several sources can be installed at a given site. The location is described by its name, coordinates and address.

S5.3 Source-ID-naming conventions in the UWO Datapool

S5.3.1 General rules for source ID nomenclature

- All **names** are lower case.
- **Transitions** are separated by "_". The alternative camelCase notation is not used, since it does not allow for machine reading of ID's.
- The **length of the character string** should be as short as possible and is limited to 40 characters (e.g.: bl_dl312_581a_wildbach = 21 characters).
- Use of **umlauts and special characters** is not permitted, except "_". E.g: Dübendorf => duebendorf
- the dominant signal is relevant in case of multiple measured signals for naming

³⁹ <https://datapool.readthedocs.io/> (data access: 15.1.2024)

S5.3.2 Nomenclature for *source ID's*

Source ID's, i.e. sensors deployed in the field have been named systematically to allow for better differentiation. The naming of source ID's consists of four parts: 1 – referenceLetters (abbreviation according to EN 81346⁴⁰); 2 - serial; 3 – manhole ID; 4 - descriptiveName. Parts are separated by "_" signs. See the following example for better explanation:

bl_dl323_rub128basin_usterstr

S5.3.2.1 Reference letters according EN 81346

Designation of every source ID starts with a letter pair "b*", whereas the pair is defined according to EN 81346 (see Table S2 below).

Table S2, left column: reference letters used in the UWO *Datapool*. *e.g. electric conductivity [mS cm⁻¹]; **also: multiple joint variables, e.g. from a compact weather station. Right column: serials of the individual sources. *** see Ebi et al. (2019) for details on the LoRa-Mesh prototypes.

ID	Variable	Unit	Serial	Source
bl	water level	[mm]	dlXXX	"DecentLab" and XXX the node-ID
bf	flow	[l/s]	fXX	"flow measurement" device with an ascending numbering per site
bs	velocity	[m/s]	plsXXXxxx	PLS-signals in general, followed by the MSR-number according to the operators
bn	rain	[mm/h]	ceXXX	the first self built LoRaWAN-prototypes followed by the last 3 letters of the LoRaWAN-EUI
bp	pressure	[bar]	lmXXX	the LoRa-"Mesh"*** prototypes followed by the numbered node-id's
bt	temperature	[°C]	rXX	rain gauges followed by an ascending numbering (note: if a device runs over a decentlablogger it's listed under "dlXXX")
bm	humidity	[m3/m3]	lpicmX	the LPICM-prototyp (Low Power Inductive Conductivity – measurement system) followed by the ascending numbering
bq	quality*	[various]	uitXX	a special temperature chain probe from the company UIT. Note: Normally all signals are in one
bx	other**	[various]	ws70X	the Lufft-WS-700 compact weather station, followed by an ascending number per device

S5.3.2.2 Serial of device

- The serial (numbers) are set according to specific device numbers or labels from the manufacturer. If no specific numbering is available an ascending number sequence is taken.

The serials used in use in the UWO-Project are described in Table S2.

S5.3.2.3 Manhole ID

- The manhole ID is taken from the municipality's sewer network cadastre.

⁴⁰ https://de.wikipedia.org/wiki/EN_81346 (data access: 20.07.2023)

- b. If the monitoring site is not documented in the cadastre as named structure, a name from a nearby object is taken, e.g. "*bn_dl802_gerber_zurcherstr*" referring to the *Gerber* garden centre.

S5.3.2.4 Descriptive Name

A *descriptive name* is allocated to the last part of the source ID to allow straightforward identification of the monitoring location in the field, i.e. where the sensor is located. Normally the following entities is referred to:

- street names,
- structure: inflow, basin or overflow - as indicator of the sensor location inside a structure,
- prominent locations, buildings nearby.

S5.3.2.5 General Rules for variables

Section S4 Sensor Classes describes the most important variables per source type. The variables contain a name, a description of the variable and a unit. The name contains an additional reference to the specific measurement location, e.g. instead of just 'temperature' it is for example 'ambient_air_temperature' or 'headspace_temperature'. Further in the description, the first part says something about the subcategory.

Here is an example:

- name: ambient_air_temperature
description: "Main measurement parameter: actual air temperature inside protective housing. Depending on the device it is ventilated or not"
unit: °C

The description further distinguishes between main/second measurement parameter, measurement quality information, internal parameter (not useful for analysis) and signal transmission information. This can help to better identify the value of the variables provided.

S5.4 Attributes for meta-data entries

Meta-data attributes are also explained in the *Datapool*. Keywords can be followed by an *action_type*. Figure S 36 below provides an overview.

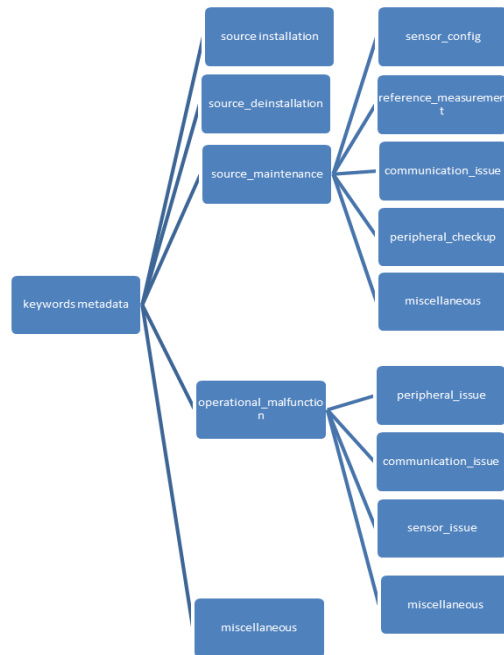


Figure S 36: Metadata keywords describing important attributes of the sensors and data

Explanation of certain categories are (meta-data log types):

- source_installation: A new data source (sensor with logger) is being installed or reinstalled after maintenance.
- source deinstallation: Removing of an operational data source (sensor with logger) also for maintenance purpose.
- source_maintenance: Events related to maintenance are logged under this category. More information under the corresponding action types, e.g. frequent checkups of a source (consisting sensor and logger) is cleaned, fixed, exchanged.
- operational_malfunction: An issue with a data source (sensor with logger), that needs to be attended to. More information under the corresponding action types.
- Miscellaneous: Events that need to be logged and do not fit the other log_types.

Action Types under source_maintenance:

- communication_troubleshooting : "Fixing of an issues of a data source (sensor) that affects data transmission or other sensor communication e.g change_antenna, replace Koax-cable, move logger position."
- Miscellaneous: Events that need to be logged that do not fall into any other action_type of the log_type source_maintenance.
- peripheral_checkup : "Any sort of in-situ maintenance tasks e.g. mechanical_cleaning, visual_checkup, data_collection, battery_change."
- reference_measurement : Logging an in situ single measurement point/parameter relating to a signal from a data source (sensor).

- sensor_config : Actions where the sensor configuration needs to be changed. e.g. change of a sensor's position, change of a measurement parameter, change sensor settings.

Action Types under operational malfunction:

- communication_issue: Issues related with transmission of the data. E.g. The data source is not reachable remotely and doesn't send data.
- miscellaneous: Issues that do not fit in any other action_types for the log_type operational_malfunction.
- peripheral_issue: Issues where is a problem between a data source (sensor and logger) occurs e.g., cable connector problems, sensor repair, antenna problems.
- sensor_issue: Issues where the source sends data which is a clearly not correct e.g., clogging, sensor moved out of measurement position.

Flag inside the dataset (separate Boolean that can be made)

- confidential_flag: Meta data entry is supposed to more confidential than others.
- low_operator_confidence_flag: Flag indicating that the data is rated as untrustworthy by the operator.

S5.5 Revised data model for *Datapool 2.0*

The data model is arranged in a star scheme (Figure S 37). In this scheme, there is one fact table which contains the measurements being stored, named signal table. The signal table is surrounded by several dimension tables which contain information about the context or attributes of the data being measured.

The variable table is the core component of data model. It contains the relational interlinkage, the measurement unit and description. To determine the variable being measured, we refer to this (variable) table. Conversely, to identify the source of the measurement, we refer to the source table. The source table is crucial as it identifies the sensor from which the measurement originates.

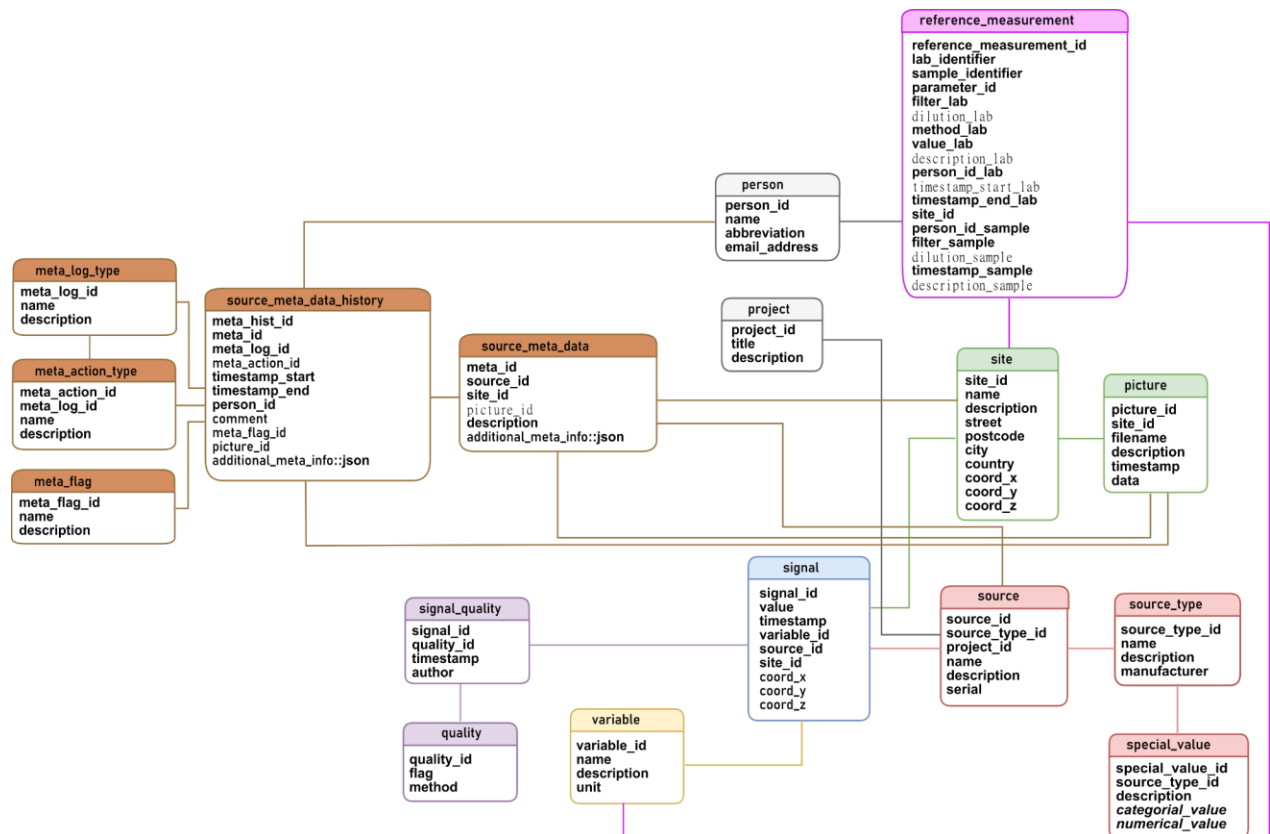


Figure S 37: Schematic illustration of the *Datapool's* data model or database layout. All data is stored in a *PostgreSQL* database so that arbitrary queries can be performed.

Further, a *source type* is explicitly defined to enable linking to the source. This is accomplished to compact the information, since one source type can have many sources. In the *source type* table, there are special values that can be defined as integer or character values. They indicate sensor readings that provide direct information from the sensor. These “special” values, such as a minus or a large negative number, indicate missing information.

The *signal quality* table links information about the signal quality, the signal, and the quality table. The quality table provides information about whether the quality flag is green or red, and which method was used to reduce the number of characters or columns. To reduce the number of columns, the information is split into tables, and a *signal ID* is linked to a *quality ID*. Additional columns such as *timestamp* and *author* capture any changes made to the method or calibration over time. The area, where all the tables are coloured black-brown, contains the meta-data which grew quickly due to the need to fit in all possible occurrences during the measurement period (years). This area contains information about the data history itself and is stored in the main *meta-data* table, where all the actions and locks are recorded, along with the time, the person responsible, and any specific information. The *lock type* table is used to bring together the specific information stored in the tables around it.

The array of old locks includes possibilities for *action type*, indicating the type of action that was performed during maintenance and similar operations. The *meta-data flag* contains information about

how the maintenance was judged by the field technician. We have the *metadata people* table, which links the *metadata ID* to the *source* or *site*. Additionally, the *metadata picture* table provides the option to store additional photographs when maintenance operations are carried out. One particular table in green is the *site* table, which is linked to a *source* and contains information about the source location.

The *site* table is also used to store information about the installation of the sensors and includes the option to save photos of the source. Reference data can also be saved in the *site* table when multiple measurements of the same *source* are carried out, such as in a lab with duplicate or triplet measurements. However, this feature is currently not used in the UWO project. Additionally, the *project* table is used to differentiate between different projects, though in our case there is only one project. The *person* table contains information about the contacts or persons who added data to several of the tables and is linked to multiple tables, as illustrated in 0.

The data model is embedded in the *Datapool* software. An illustration of the whole software environment is shown in Figure S 38.

Datapool - Store time series, meta data and much more

Christian Förster¹, Uwe Schmitt², Frank Blumensaat^{1,3}, Simon Bloem¹, Andy Disch¹, Jörg Rieckermann¹

The Datapool is the Eawag's and SIS's approach to an easy to set up and use, modern data warehouse for structured data. It offers a clear separation of data management roles (admin, provider, user). With usability in mind, queries run fast even for large amounts of data. The datapool's core components enable high interoperability with other software.

Currently the datapool is used in various different projects at Eawag and ETH. The most data intensive projects reach **~2 billion rows** (Water Hub at NEST) and **~0.7 billion rows** (Urban Water Observatory) in the main table.

Operation

- Secure functioning via user management / workflow / data checks
- File drop (landing zone) for fast automated data ingestion from various sources
- Dashboard for monitoring system performance and health
- Controlled vocabulary for maximal flexibility while ensuring consistent data

Database

- Structured in a snowflake schema
- Storage capability for time series, meta data, signal quality information, binary data, raster data, laboratory data
- Performance for simple query: 100 million data points takes 10s (data shape: ~11.2 million x 9, table length: ~0.7 billion rows)

Accessibility

- Source code on [GitLab](#)
- Datapool's Command Line Interface
- Grafana Dashboard
- Documentation on [readthedocs.io](#)
- Clients with predefined queries for Python, R, Octave, MatLab, (Julia)
- Other (eg.: [uwo-opendata.eawag.ch](#))

Components

The software's main data storage utilizes PostgreSQL with the PostGIS and TimescaleDB plugins. System data for monitoring purposes is stored in Prometheus. For data visualization and analytics as well as system monitoring Grafana is included in the datapool's package suite. Ansible and Docker simplify testing and deployment of the system. Currently Python, Julia and R are the programming languages supported for data conversions.



Science that matters

¹ Department of Urban Water Management, Eawag
² Scientific IT Services, ETH Zürich
³ State Directorate Saxony, Germany

Figure S 38: Schematic illustration of the Datapool warehouse, including the data processing and storage pipeline. © OpenStreetMap contributors 2024. Distributed under the Open Data Commons Open Database License (ODbL) v1.0. (map in www.uwo-opendata.org)

S5.6 Tracking issues in the UWO dataset using a version control system

Tracking changes in a dataset is crucial, especially when sensor artefacts or periods of sensor malfunctioning are discovered, or reliability issues with a sensor are identified. Also, data quality problems should be documented, e.g. through tracking of artefacts and features, e.g. timestamps of anomalies. Most of all, the documentation of data manipulations and quality control efforts, as well as clear communication are vital to maintaining reliability. While other communities solve this issue by setting up dedicated webpages⁴¹ to document artefacts and features in common datasets, is still uncharted territory in the urban drainage community and how to best track issues as well as corrections is unclear.

Instead of documenting this on a dedicated webpage, we created a public GitLab repository⁴². While this does not enable us to continuously produce new, corrected versions of the observations, we hope that it facilitates the documentation of issues and identification of viable solutions by allowing the tracking of changes, and leveraging issues for tracking and addressing specific problems. We believe that a versioning system's features contribute to effective management of quality control and artefacts in the UWO data, providing a transparent and well-documented history of suggested dataset modifications and resolutions.

⁴¹ <https://jwst-docs.stsci.edu/data-artifacts-and-features>

⁴² Gitlab repository to track and document issues with the UWO dataset: <https://gitlab.com/uwo-eawag/> (data access 15.1.2024)

S6 Dynamic plot of the data completeness

To better assess the usefulness of the dataset, we provide an interactive figure in html format (cf. browser screenshot in Figure S 39) to explore the data completeness in weekly granularity. It shows the level of completeness of the data on a scale from 0 (all data missing - white) to 1 (all data available – dark blue) from 01.01.2019 to 31.12.2021. Data package A1 = precipitation sensors; A2 = hydraulics sensors; A3 = temperature data; A4 = LPWAN sensor nodes. The light blue colour indicates that fewer data points have been collected than expected, either due to sensor failure or incomplete transmission. The dynamic plot is available in package C.

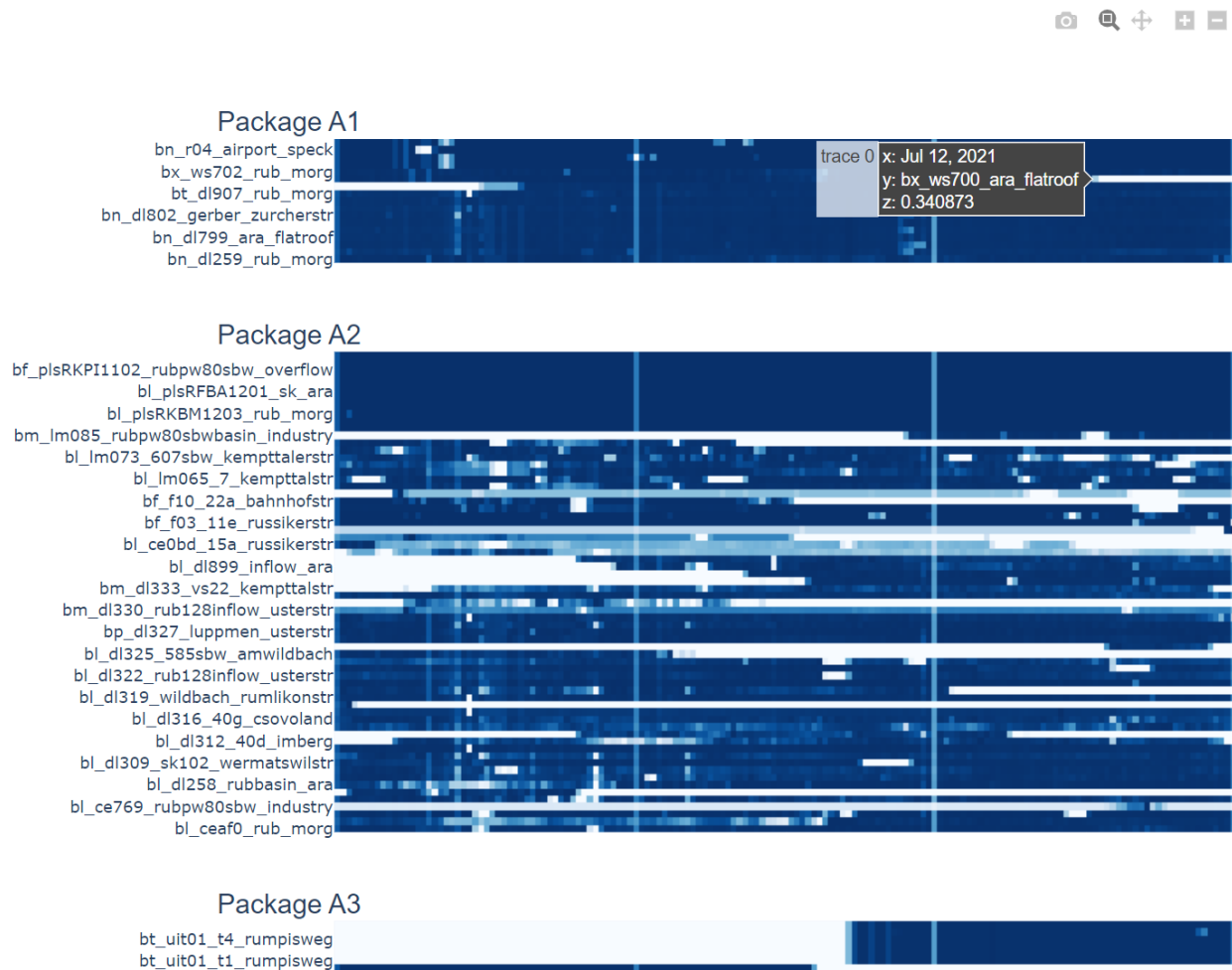


Figure S 39: Browser screenshot of the interactive plot to explore the completeness of the data packages A1-A4. Dark patches indicate weeks in which data points could be collected regularly. White patches indicate periods where data are completely missing. For example, the screenshot above shows that the weather monitoring station WS700 on the roof top of the WWTP [`bx_ws700_ara_flatroof`] ceased operation on 12 July 2021.

S7 Hydrodynamic sewer models

S7.1 Hydrodynamic sewer modelling

Hydrodynamic sewer modelling is a computer-based calculation method to predict rain-induced surface runoff and wastewater transport during dry and wet weather periods in the corresponding collection system. It takes into account various factors such as the size and cross section geometry of pipes, the topography of the area, and the flow rates of sewage to predict the behaviour of the wastewater as it travels through the network. This information can be used to optimize the design and operation of sewer systems and to identify potential issues before they occur.

S7.2 Sewer network implementation in EPA SWMM

Model evolution: Krejci et al. (1994) reported a very first hydrological sewer model implemented in DHI MOUSE⁴³, as well as a simplified model of the trunk sewers to speed up computations. Starting point for the development of the provided SWMM model was a hydrodynamic model implemented in MikeUrban⁴⁴, a commercial, off-the-shelf hydrodynamic sewer modelling platform. This MikeUrban model was established within the scope of the urban drainage master planning (Hunziker-Betatech, 2016). This model was implemented in EPA SWMM⁴⁵ (EPA, 2021), which allowed for an open-access version of the model. The conversion revealed structural discrepancies regarding flow topology and weir configurations. These 'structural errors' were corrected manually. The here provided base model considers only the combined part of the sewer system; the stormwater sub-systems that directly discharge into adjacent rivers have been ignored (cf. Figure S 40). It therefore considers 246 sub-catchments that drain into 427 junction nodes connected by 431 links, with six overflow structures of which four have a notable retention volume (see Section S3.1).

Over time (2016 – ongoing), the model has been thoroughly revised, and the hydrological and hydraulic parameters have been adjusted. The construction characteristics of the sewer pipes have been checked for representativeness. However, pipe and manhole geometries have been widely left unchanged from the MIKE Urban model, as this information had been taken from the official municipal cadastre. Dry weather flow rates, storage tank characteristics including storage curves, as well as pump curves and pump control were verified during model revisions.

Infiltration of groundwater and rainwater: in the Fehraltorf system infiltration into sewers plays an important role for the flow conditions during dry weather as it may vary considerably depending on the season. In the base model provided, the groundwater infiltration (GWI) is considered through external flow inputs (GWI rates) derived from night-minimum flow analyses of the measured WWTP inflow rate.

⁴³ [https://en.wikipedia.org/wiki/Mouse_\(software\)](https://en.wikipedia.org/wiki/Mouse_(software)) (data access 30.11.2023)

⁴⁴ <https://www.mikepoweredbydhi.com/products/mike-urban> (data access 30.11.2023)

⁴⁵ EPA SWMM, release used: 5.1.013 - <https://www.epa.gov/water-research/storm-water-management-model-swmm> (data access 30.11.2023)

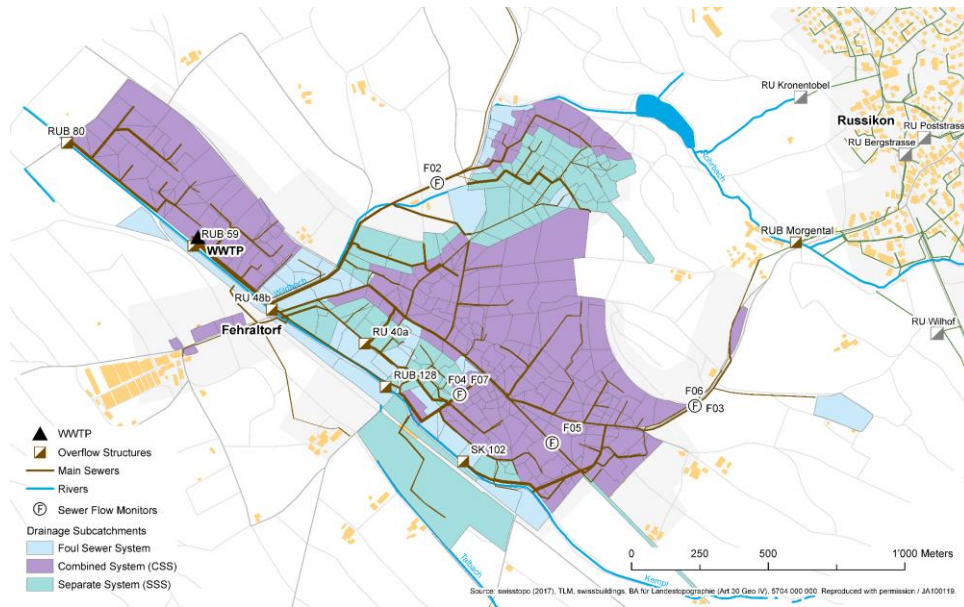


Figure S 40: Separation of the catchment into parts draining via combined system (purple) and separate system (light blue and mint). Sanitary sewers carrying only foul sewage are implemented in the model, while storm sewers that discharge directly into adjacent rivers are not. It is important to note that the colour-shaded areas and corresponding network elements are included in the hydraulic base model. Source: ©Swisstopo (2017), TLM, swissbuildings, BA für Landestopographie (Art. 30 Geo IV), 5704 000 000 Reproduced with permission / JA 100119

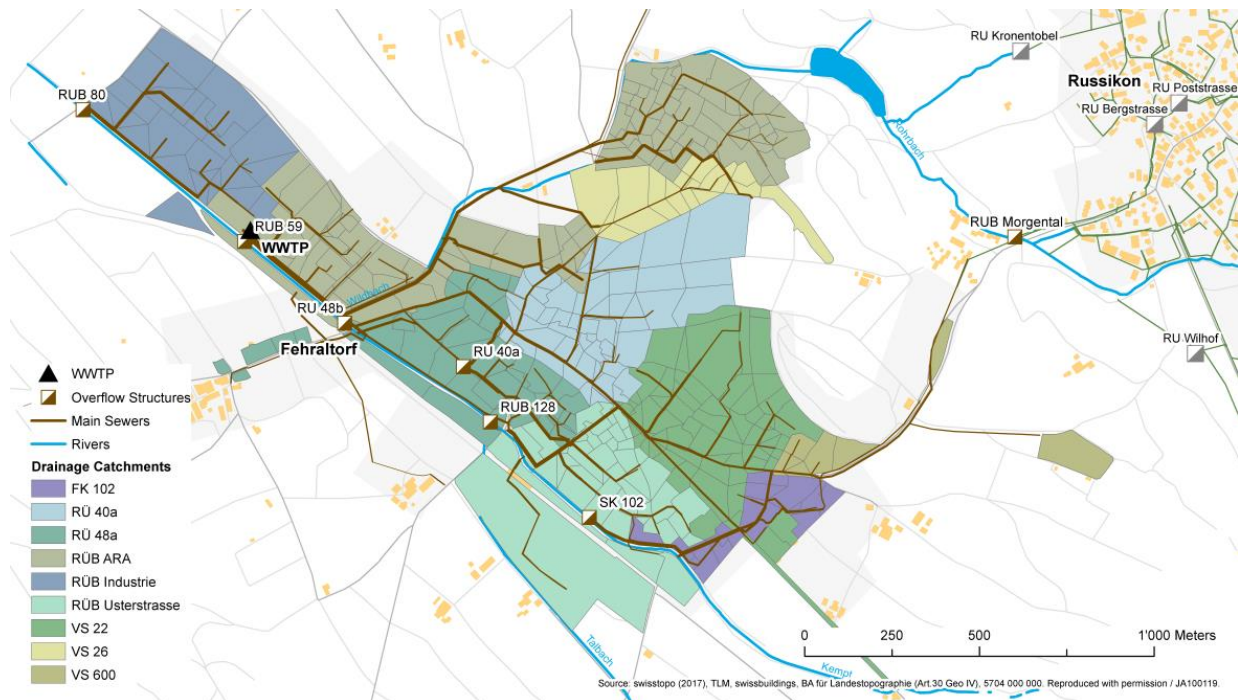


Figure S 41: Differentiation of CSO sub-catchments in the Fehraltorf combined sewer system. Source: ©Swisstopo (2017), TLM, swissbuildings, BA für Landestopographie (Art. 30 Geo IV), 5704 000 000 Reproduced with permission / JA 100119

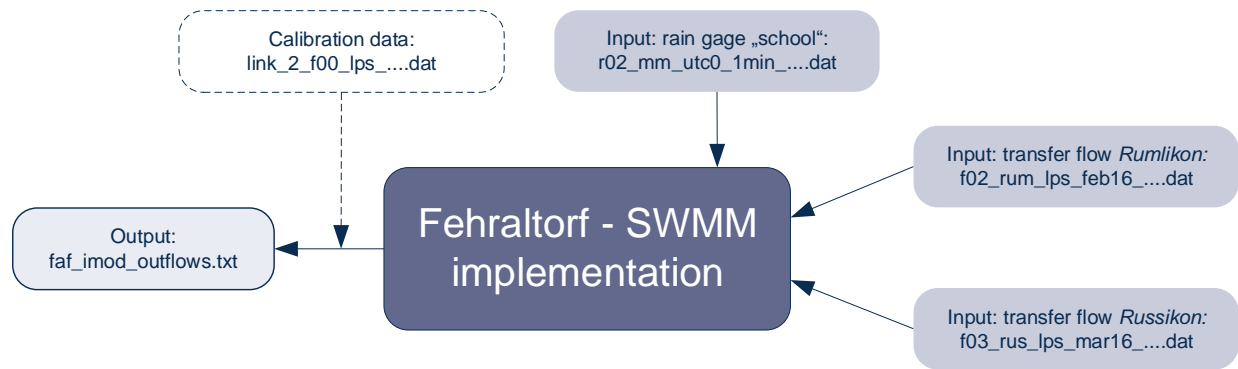


Figure S 42: Schematic description of the sewer network model (base model), including input and reference data files provided in package B2.

The implemented GWI rates vary on a monthly basis, i.e. monthly factors are applied to constant base rate which is assumed to be equally distributed across all the nodes in the network. This assumption can be further refined, e.g. based on recent findings (Ramgraber et al., 2021) – see Section S9.2 . Moreover, the base model includes a hypothetical catchment area producing slow rain-induced runoff. This flow component, also known as rain-induced infiltration (cf. Staufer et al., 2012) is mimicking the typical lag flow after rain events.

Transfer flows: Fehraltorf’s wastewater system has two inflows as upstream boundary conditions, the transfer flows from the two neighbouring municipalities *Rumlikon* and *Russikon*. In the given model implementation these inflows are represented as measured inflow time series, i.e. data collected within the scope of the UWO initiative and for the period from 2016 to 2022 (c.f. Figure S 40). In the scope of this open data paper, simulations using these measured transfer flow inputs are therefore limited to this specific period. Nevertheless, two simplified SWMM models for the neighbouring villages are provided to extrapolate flows outside the window of measurements (*rum.inp* and *russ.inp*).

S7.3 Adjustment of the SWMM model to observations

The **base model** (model provided in package B2): After conditioning the model for dry weather using the measured WWTP inflow as reference, the first wet-weather adjustment of the model was based on the recommendations by Schmitt *et al.* (2008), i.e. by checking the volume balance against the WWTP inflow rate for several non-extreme rain events. The base model predictions show a reasonable alignment with observations, which has been tested for WWTP inflow and four additional locations in the sewer network during the calibration period from March to May 2016 (Figure S 43). The goodness of fit of the model was assessed using flow observations in terms of i) bias, i.e. the ratio of modelled and measured cumulative flow, and ii) the Nash-Sutcliffe efficiency (*NSE*) coefficient (Figure S 43).

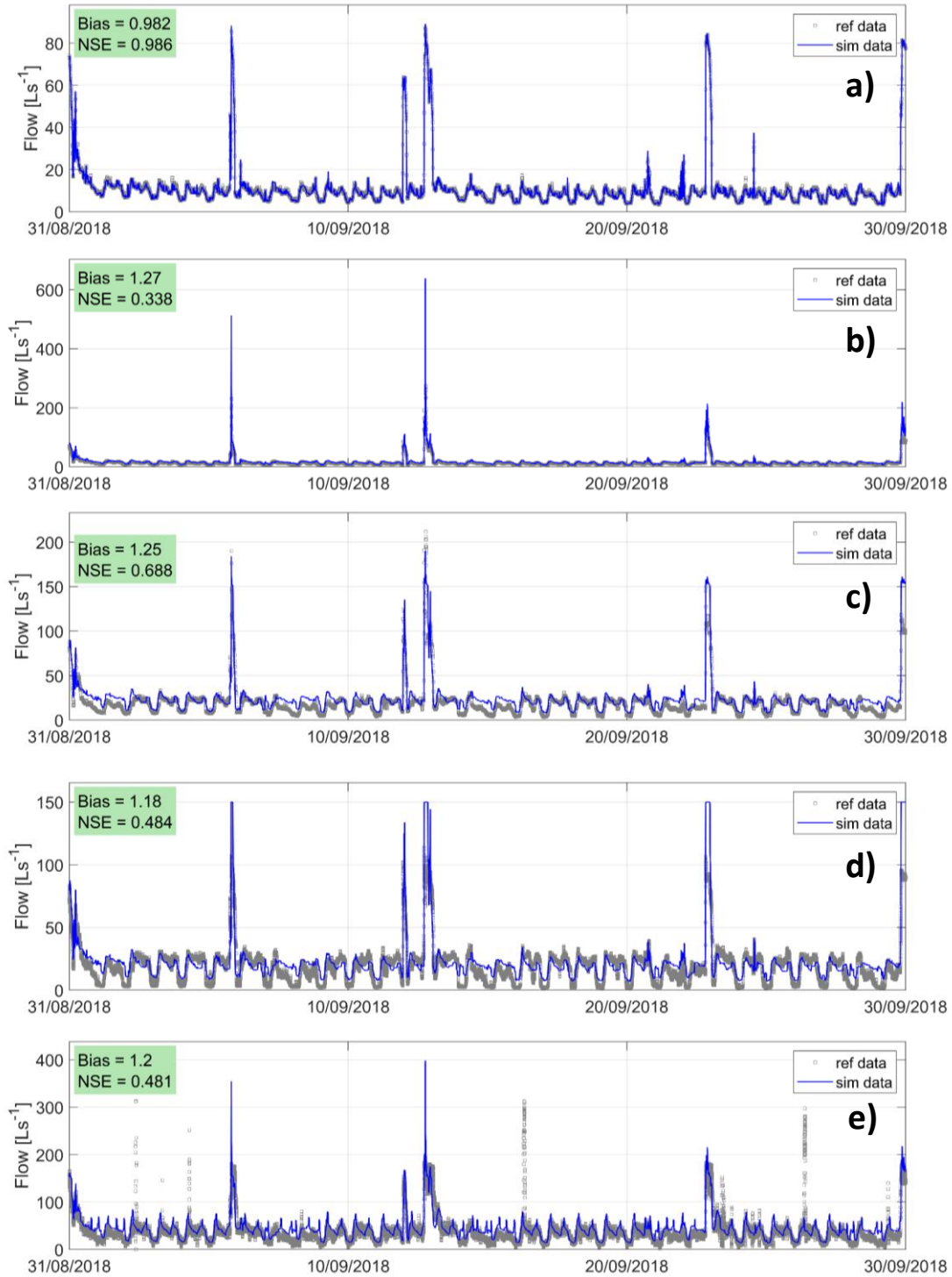


Figure S 43: Modelled vs. observed flow with the base model at several locations in the Fehraltorf sewer network for a period of one month on September 2018. Locations (top -> down): a) f03_11e_russikerstr, b) bf_f07_23_bahnhofstr, c) bf_f08_166_luppenweg, d) bl_ceb60_138a_venturi, e) catchment outlet, i.e. WWTP inflow -> bl_d1257_inflow_ara (SWMM node: Link_2). Validation period: 30 days in September 2018. Bias here is defined as difference, i.e. ratio of modelled and measured (cumulative) flow.

S7.4 Past and current developments of the SWMM model

The provided base model SWMM is continuously being adapted to meet ongoing research needs.

Model used in Wani et al. (2017): Using three different flows of the main collector in the Fehrltorf system (upstream, midstream and entry to the WWTP), (Wani et al. 2017) performed a spatial calibration of the SWMM model using the Bayesian parameter inference approach and the NSE as the different points as objective functions. The rainfall period consisted of two rainfall events, over a 50-hour duration. They concluded that the calibration of the model using spatially distributed data did not lead to better parameter estimates in Fehrltorf. They attributed this to the fact that: i) the flow measurements are primarily taken in the central collector, which does not provide information (i.e. the variability) on the subcatchment behaviour upstream, (ii) the presence of throttles that suppress rainfall-runoff signals downstream, and finally, (iii) uncertainties related to the collected data (Wani et al. 2017).

Model used in Joshi et al., 2021: The result of (Wani et al. 2017) was further explored by manually calibrating the same subcatchment variables, but using a longer two-year rainfall period between February 2016 and June 2018 (Joshi et al., 2021). Both calibrations obtained NSE values of over 0.5 for the WWTP inflow during the calibration, which is considered satisfactory (Moriassi et al., 2007). Refer to Joshi et al. (2021) for details on the results of the calibration and validation.

Model used in Rodriguez Bennadji (2022): The implementation used in Rodriguez Bennadji (2022) includes: i) integration the aquifer and groundwater module, ii) change of the soil infiltration module to the Green-Ampt model. This version also provides additional capabilities by developing data-driven models to predict continuous transfer flows. The parameters governing the surface runoff processes were also checked and updated based on the latest GIS data (2022) available.

For the transfer flows from Rumlikon and Russikon, a machine learning model for each boundary flow was developed based on rainfall and other relevant variables, which makes it possible to predict inflows for historical and future climates. These options are not part of the base version provided in the open-data publication.

For infiltration, the SWMM model was modified to better represent dynamic infiltration. In the first version, infiltration was modelled using an aquifer and groundwater module. For the first implementation, the parameters estimated by Joshi et al. (2021) were re-calibrated to include the updated imperviousness. The calibration uses the normalised NSE (nNSE) at two points in the main collector (midstream and inlet of the WWTP) as objective functions and calibrates parameters related to the hydrological characteristics of the surface.

Alternatively, a second implementation was developed, where twelve parameters were calibrated in the groundwater and aquifer module, as these values are unknown due to a lack of data on the soil and aquifer characteristics in Fehrltorf. In addition, in addition to *bias* and *NSE*, two objective functions using the groundwater table data were included in the optimisation. The model parameters were automatically re-calibrated using a multi-objective evolutionary algorithm, NSGA-II (Deb et al. 2002). The calibration period

ranges from May 2018 to April 2019, while the validation period lasts from May 2019 to April 2020. Both versions of the model perform well in the calibration and validation period, with NSE being over 0.5 for flow at the inlet of the WWTP. More information about the final calibration and validation results can be found in Rodriguez Bennadji (2022).

Ongoing and future model developments include integration of the stormwater drainage system and a coupling with a surface 2D model. Similar as with the versioning of the data, these will be made available through our code repository⁴⁶.

⁴⁶ <https://gitlab.com/uwo-eawag/>

S8 Exploring operational challenges: lessons from operating a full-scale field laboratory for urban drainage monitoring

In this section, we aim to delve into the multifaceted challenges of operating a full-scale field laboratory. A team of three to eight members of the Eawag Urban Drainage Department (none of them full-time) has been operating the Urban Water Observatory in Fehraltorf since 2015. As an academic institution - rather than a provider of engineering services - this presents several challenges, from collaboration with municipal utilities, internal teamwork and issues of work safety, and maintaining data quality in sewer monitoring equipment. Addressing these more practical “lessons learned” systematically, we provide insights and solutions, offering a guide for researchers navigating the complexities of field laboratory operations.

S8.1 Co-operation with the municipal utility and communication with the public

Even with the best equipment and the most skilled personnel to maintain it, a campaign will fail without the support of the local operator. It is invaluable to communicate regularly with the utility company, to provide information in the form of reports and monitoring results, and to act respectfully and reliably at all levels of qualification. The excellent cooperation with the municipality of Fehraltorf and the municipal water utility has been a key factor in the success of the UWO.

Effective communication also includes informing relevant stakeholders and the general public about the results achieved and the work in progress. While many long-established observatories use their website to communicate news, project results and openly available datasets⁴⁷, we have had very good experience with the timeline format, which provides a chronological and easily accessible overview of achievements⁴⁸.

S8.2 Internal collaboration, knowledge management and work safety

In an academic environment, field laboratories often have limited resources and must cope with significant turnover of students, post-doctoral fellows, researchers and other staff. This can make it difficult to carry out certain experiments or analyses and puts additional emphasis on knowledge management. **Precise and consistent documentation**, i.e. following maintenance protocols, documenting activities in an operating logbook ensures that important information does not get lost, even if operating personnel changes. A web-based wiki system may help to facilitate documentation while work is done in the field and helps to acquire sensor metadata (cf. Section S8.4) and actual information about the lab status from anywhere.

⁴⁷ <https://ddp.tereno.net/ddp/> (data access 23.10.2023)

⁴⁸ <https://www.tiki-toki.com/timeline/entry/1913653/Urban-Water-Observatory/> (data access 23.10.2023)

The batch-wise rollout of sensors is key for a successful deployment of a large number of interconnected sensors. Allow sufficient time after installation to monitor the performance of each batch of sensors deployed and make any necessary adjustments. Deadline-driven rollouts with over-ambitious targets run the risk of high maintenance efforts, frustration, and poor data quality. It took us a few years, but with hindsight we would not have done it any faster, given the limited resources available.

Safety must be a top priority during implementation: urban drainage field labs raise safety concerns, particularly due to the extreme environment with harsh conditions, such as toxic and explosive atmospheres, limited access, often in the middle of traffic, infectious pathogens, and physical hazards such as confined spaces or slippery surfaces. Therefore, it is important to take appropriate precautions to ensure the safety of all personnel involved, even if this makes it difficult to maintain equipment or carry out experiments.

S8.3 Sewer monitoring equipment, sensor choice and the challenge of maintaining good data quality

Urban drainage field laboratories often face challenges in maintaining data quality, particularly when working in remote or difficult-to-access locations. This can include issues with sample collection, storage, and analysis, as well as difficulties in maintaining consistent protocols across multiple research sites.

Using low-cost, IoT-enabled sensors extends the possibilities to capture spatial variability, but it does not make traditional monitoring with just a few high-precision monitors obsolete. We have learnt it pays to establish a monitoring backbone consisting of a few full-featured, more accurate but (often) maintenance-intensive sensors (in-sewer flow; rainfall). Because of their high measurement accuracy, the data can be used as reference observations, and the data allow reliable volume balancing.

Furthermore, it should be investigated whether the overall data quality can be improved by temporarily monitoring one and the same process variable with yet another source signal to obtain so-called proxy-signals (e.g. stage-discharge relation).

“Plug ‘n pray” approaches may work in a few cases, but a careful sensor deployment in the field, coupled with a balanced mix of routine and on-demand maintenance (enabled by real-time data transmission) is one, if not the, most efficient way to enable the collection of high-quality data.

A-priori testing of ‘to-be-installed’ sensor systems under lab conditions is extra work but is a much less time consuming as when you “get to know” your sensor system in the field. Handling 100+ sensors in a research environment efficiently requires dedication, pragmatism and the willingness of on-call service availability on an irregular basis. After five years of sensor network operation, we had managed to reduce maintenance time to on average eight man-hours a week. The main cost factor is clearly not the investment in monitoring equipment, but the effort put into operation and maintenance of this equipment.

Urban water field laboratories often rely on specialized equipment that can be expensive to maintain and repair. It is important to have a robust maintenance plan in place to ensure that equipment is functioning properly and to minimize downtime.

A-posteriori data validation may be as sophisticated but it will not compensate for carelessness during installation or the lack of adequate meta-data (Russo et al., 2021, p. 21).

Automated data validation is essential for a larger number of sensors (> 30-40), it helps to reduce the effort spent on sensor maintenance, but it cannot replace regular, more advanced analyses of data, i.e. in a longer temporal context and in connection with neighbouring sensor signals. Ideally, the ultimate data user himself follows up the data collection campaign and evaluates sensor readings at regular basis. Unfortunately, this is not possible, among other things because millions of labelled datasets are lacking. As even we experts are struggling, automated data validation and assessing sensor uncertainty is a current research topic in the urban drainage community.

In addition, compliance with ATEX regulations is required to minimize the risk of explosions in sewer environments and ensures the safety of workers, equipment, and the surrounding infrastructure. It is essential to consult relevant local regulations and guidelines specific to the area of operation to determine the specific ATEX requirements applicable to sewer systems.

However, ATEX compliance may not always be practical in research projects for i) alternative safety measures and ii) practical constraints:

i) Safety Considerations: Research projects in sewers must prioritize the safety of personnel and equipment. While ATEX compliance is essential for working in potentially explosive environments, research activities may be limited to non-hazardous areas or involve non-intrusive methods that minimize the risk of ignition sources. In such cases, alternative safety measures may be implemented instead of full ATEX compliance. The temporary application of low-power (< 3.6 Volts) technology is one option to reduce the efforts while still complying with rather stringent ATEX rules.

ii) Practical Constraints: Research projects often face practical constraints such as limited time windows, budget restrictions, or the need for flexibility in experimental deployments. These factors may make it impractical or infeasible to ensure full ATEX compliance within the constraints of the research project.

S8.4 The importance of metadata

Meta-data are essential to correctly interpret sensor signals. Meta-data collection must not be neglected, neither during routine nor during on-demand maintenance. Standardized maintenance protocols help to ensure a consistent and efficient meta-data collection. With this regard, semantics of sensor IDs (naming) should be determined a priori: unique, flexible enough to accommodate various eventualities (new sensor types, sensor shifts), non-cryptic so that ad-hoc identification of sensor and monitoring location is possible.

To improve the interoperability of urban drainage field data, modern approaches to data exchange and data annotation, the research community should develop an ontology of urban wastewater systems. This is well established in other fields to unambiguously define compartments and helps to communicate a lot of information e.g. for data collection. Good starting points for international accepted standards would be the Dutch GSWS⁴⁹, the ontology developed in the CD4WC project (Koege et al., 2007), urban

⁴⁹ <https://data.gsws.nl/>

infrastructure-oriented ontologies as – for instance – outlined in (Du et al. 2023), or potentially the EnvO⁵⁰, which is a community ontology for the concise, controlled description of environments.

S8.5 Telecommunication and data transmission

Field laboratories may be in areas with limited or no communication infrastructure, which can make it difficult to stay in contact with other researchers or to share data in real-time. This can lead to delays in decision-making and coordination between research teams.

We found that transmitting the data from underground structures remains a challenging factor for every site where some improvements over time needs to be implemented.

⁵⁰ <https://sites.google.com/site/environmentontology/>

S9 Research opportunities

This section provides a more detailed description of Section 4 of the main manuscript. For ease of reference, the references are summarised in a common list at the end of the SI.

S9.1 Anomaly detection of sewer monitoring data using semi-automated machine learning approaches

Rapid ongoing developments in the field of sensor technology and data transmission enable a cheaper and more flexible process monitoring in drainage systems than ever before (Kerkez et al., 2016; Ruggaber et al., 2007). This generates significantly more data. With historical methods (i.e., predominantly manual data preparation and checking) we will fail in efficiently extract useful information.

Fully or semi-automated approaches are required to enable robust real-time sensor data validation while allowing human intervention to improve the quality of the data. Fair results can already be achieved by applying rather simple methods to process monitoring data of low-level complexity (Deheer, 2022). Nevertheless, they are limited when examining several signals of different types in real-time, such that computationally expensive analysis methods are to be used. Machine learning (ML) methods, especially those for unsupervised learning, promise a step-change in real-time data preprocessing and promise a timely, coherent, complete assessment of data quality (Aggarwal, 2017), which gets more efficient with increasing amount of data. The quality of the recorded data can be assessed by detecting and flagging anomalies, i.e. the deviation from the "normal" (Branisavljević et al., 2010).

A benchmark study comparing the performance of different validation routines on different environmental field data sets revealed that i) pre-processing of raw data is essential, ii) existing advanced validation methods fail when applied to urban drainage raw data (Russo et al., 2021).

Here, we compare three data validation methods (ARIMA, Autoencoder and One-class SVM) and compare their performance for observed time series from the UWO dataset with different degrees of pre-processing. We consider three pre-processing steps including filtering (A), smoothing (B) and imputation (C).

As a reference, we use the predicted time series of a hydrodynamic rainfall-runoff model, which is spiked with realistic, but synthetic errors (D). Different types of synthetic errors are added, including point anomalies, drifts and freeze. These anomalies are randomly distributed across the simulation suites with a proportional occurrence in training and test data sets. This time series is used as the basis of a benchmark for the different automated anomaly detection algorithms.

As a performance metric, we chose the F1 score, which describes a model's accuracy on a dataset. It is often used to evaluate binary classification systems, which classifies examples into 'positive' or 'negative' (here: "normal" or not). It is a popular metric because it provides robust results for both balanced and imbalanced datasets.

$$F_1 \equiv 2 * (Precision * Recall) / (Precision + Recall)$$

where *Precision* measures how accurate the ‘positive’ predictions of the model are. A high precision score means that the model has a low number of false positives and is good at identifying the relevant instances. *Recall* measures show how well the model can identify all ‘positive’ instances in the dataset. A high *Recall* score means that the model has a low number of false negatives and is good at finding all relevant instances (Hastie et al., 2009). Scores of < 0.5 are generally considered low.

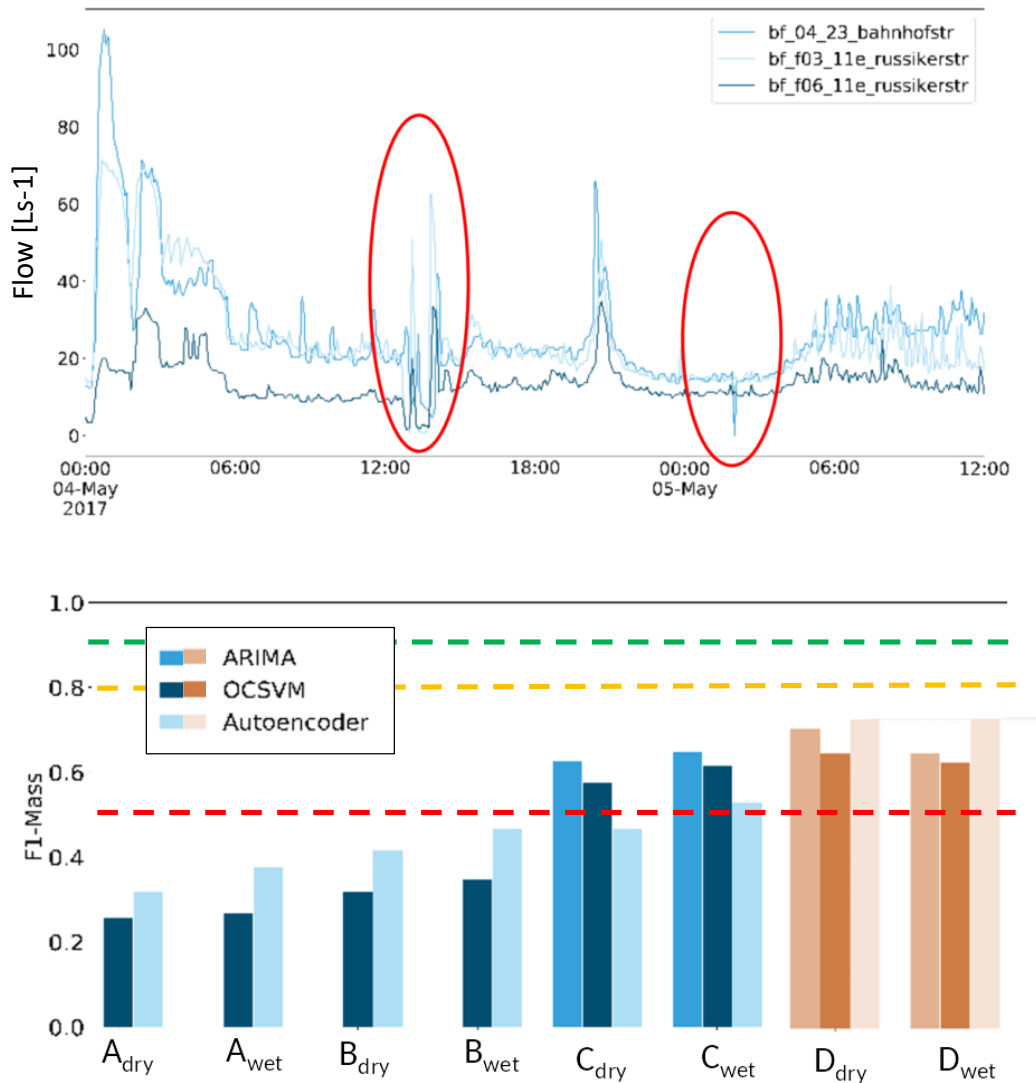


Figure S 44: Top: Observations with potential anomalies. The highlighted data show the benefit of multiple sensors in detecting anomalies. While the high variability on the left is reflected in all sensors, the one on the right only appear in a single sensor. Bottom: F1 scores for different methods for pre-processing (A-D). An F1 score of 0.5-0.8 (between the red and yellow dashed lines) is considered medium quality, 0.8-0.9 good and above 0.9 excellent. For real-world data (blue, A-C), the performance increases with increasing levels of pre-processing. For real world data, ARIMA performs best and the Autoencoder never reaches the performance on synthetic data (red, D).

A low F1 score means your classifier has a high number of false positives which can be an outcome of imbalanced class or untuned model hyperparameters.

First, it can be seen in Figure S 44 (top) that analysing several related signals simultaneously makes it possible to detect sensor anomalies (missing correlation in related signals, e.g. right circle). Second, the F1- score is higher, the more the data was pre-processed by human intervention.

For the synthetically generated time series during wet weather, we obtain an F1 value of 0.71 for the ARIMA, 0.65 for the OCSVM and 0.73 for the autoencoder. In dry weather, the performance score is resp. 0.65, 0.63 and 0.73 in dry weather. These values are higher than all scenarios with real measured data. On average, the synthetic scenarios have an F1 value of 0.68 and the ones based on real-world observations have an F1 value of 0.43. As expected, the F1 score for dry weather is only slightly better, on average 0.07, than that for wet weather for all algorithms and scenarios.

As expected, our results demonstrate that the F1 value increases with the degree of data pre-processing. For example, de-noised, smoothed, padded data (imputed) are best for detecting anomalies. Also, applying the ARIMA method fails for all incomplete series ($F1=0$). Our results also suggest that splitting the data into dry and rainy weather can enhance performance by enabling more effective anomaly detection. Therefore, refining the algorithm architecture for this purpose could have a significant impact on results. While ARIMA and Autoencoder methods show promise with minimal calibration effort and synthetic data sets, their dominance over OCSVM is less pronounced when using real measurement data.

The initial results of the exploratory method comparison on selected flow data indicate that the effectiveness of the method heavily relies on the data processing technique employed. As such, developing effective processing techniques for sewer monitoring data will be crucial for accurate analysis and interpretation of the data, especially in the absence of widely available labelled datasets. Unlike other areas such as text archives or annotated photos, there is, to the best of our knowledge, no labelled monitoring data available for sewer systems (Deheer, 2022). Traditional human-assisted labelling methods like CAPTCHA and artificial AI are also challenging to implement due to difficulties in identifying sensor failures, even for experts (Disch, 2022; Fraternali et al., 2012).

S9.2 Quantification of groundwater infiltration

Infiltration, or extraneous water in urban drainage systems is undesirable water that can reduce the efficiency of wastewater treatment and increase costs for conveyance and treatment. It dilutes sewage during dry weather, and it can lower the temperature of raw wastewater, both of which reduce the efficiency of biological treatment. It also puts extra load on the drainage system during rain, using up capacity and causing extra costs to transport, buffer, and treat the increased volume. Groundwater infiltration is one of the most significant sources of extraneous water, which can vary depending on the season, pipe deterioration, and groundwater levels.

We estimated groundwater-infiltration (GWI) rates in the Fehrltorf sewer network with a systematic separation of flow components in long-term flow recordings (Staufer et al., 2012). This focuses on separating dry weather night-minimum flows and excluding rain-induced infiltration (RII) components. In periods of stable dry weather, we assume that in-sewer flow at night consists of i) a minim amount of foul

sewage and ii) groundwater that infiltrates through deteriorated sewer pipes, leaky pipe joints. The night-minimum flow is assumed to occur at night-time from 02:00 to 04:00, depending on the monitoring location and corresponding travel times in the system (Hager, 1999). The minimum amount of municipal foul sewage (FS) can be estimated either based on per capita specific discharge rates ($q_{FS,min} = 0.3 - 1.0 \text{ L s}^{-1} 1000 \text{ cap}^{-1}$) or as percentage (5-10 %) of the daily mean of the municipal FS flow, estimated through the number of inhabitants and water consumption statistics. Using a long time series from 2016 until 2020 and assuming a percentage of 5 %, results in a foul sewage night minimum of 1.1 L s^{-1} at the inflow of the central WWTP (0).

Table S3: Key figures for foul sewage night minimum and groundwater infiltration flows at three locations in Fehraltorf (F00). Water consumption estimate for central Fehraltorf, differing from estimates for neighbouring catchments Russikon (F03) and Rumlikon (F02). The ID of the flow monitor location corresponds to the hydrological flow scheme and/or the monitoring layout.

Flow measurement location	F00 (WWTP)	F02 (Rumlikon)	F03 (Russikon)
Inhabitants ⁵¹ [-]	6500 (+4000 ⁵²)	600	3400
Per capita water consumption [$\text{L cap}^{-1} \text{ d}^{-1}$]	187 (158)	158	158
<i>per capita</i> specific discharge ($q_{FS,min}=0.3$) [L s^{-1}]	3.30	0.30	1.02
5 % of average foul sewage discharge [L s^{-1}]	1.11	0.11	0.37
GWI range [25%ile (median) 75%ile] in L s^{-1}	16.0 (17.4) 22.5	1.34 (1.53) 2.25	3.88 (4.45) 5.22
GWI concretely for Apr 2019 (exemplary period)	20.9	1.5	6.4

We used the night-minimum flow to estimate GWI rates in the Fehraltorf sewer network at the catchment outlet and two transfer flows from the Rumlikon (F02) and Rumlikon (F03) catchments. GWI rates are presented as median with interquartile ranges (Table S3) to reflect seasonal variability. The analysis allows quantifying the “inner” infiltration within the Fehraltorf catchment, excluding imported groundwater upstream of F02 and F03. This ranges from 10 to 15 L s^{-1} depending on the season. Infiltration dynamics are illustrated in 0, using the WWTP inflow as an example.

In addition, the spatially detailed monitoring data show that the spatial extend of GWI varies with the seasons (Ramgraber et al., 2021). Figure S 46 illustrates that in April 2018 (left), with a comparably high groundwater table, 256 of 459 manhole inverts are located below the groundwater table, whereas in October 2018 (right) only 100 manholes are affected. In the future, the estimated GWI rates can be implemented as spatially differentiated input in the accompanying hydraulic sewer network model (see Section 3.3 in the main manuscript). In the given model implementation, the “inner” Fehraltorf infiltration rate is homogeneously distributed, i.e. an equal share is assigned to each model node.

⁵¹ <https://www.web.statistik.zh.ch/gpv2/> (data access 20.07.2023)

⁵² Person equivalents from non-residential discharges

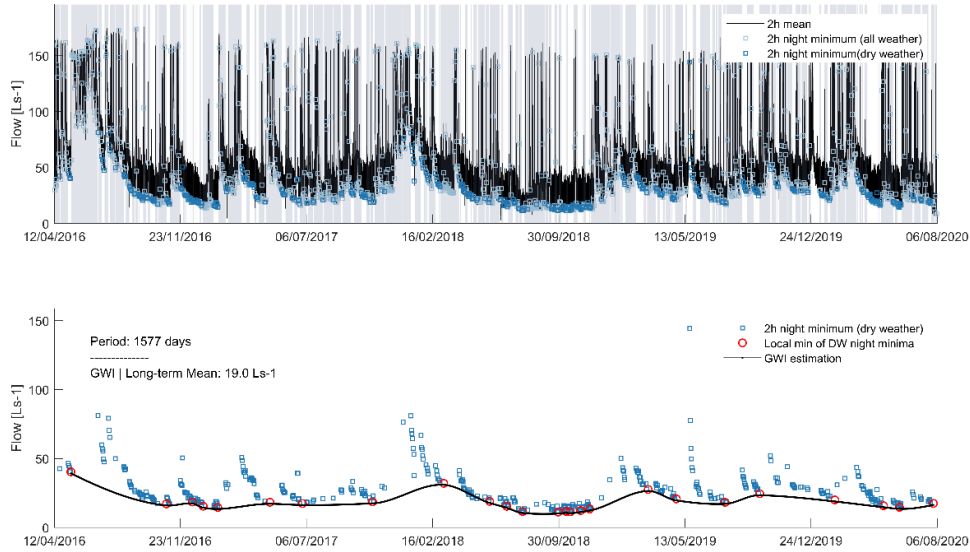


Figure S 45: Top: inflow to the WWTP Fehraltorf (F00) as 2h-averages. Bottom: Groundwater sewer infiltration rate (black line) based on dry-weather night minima.

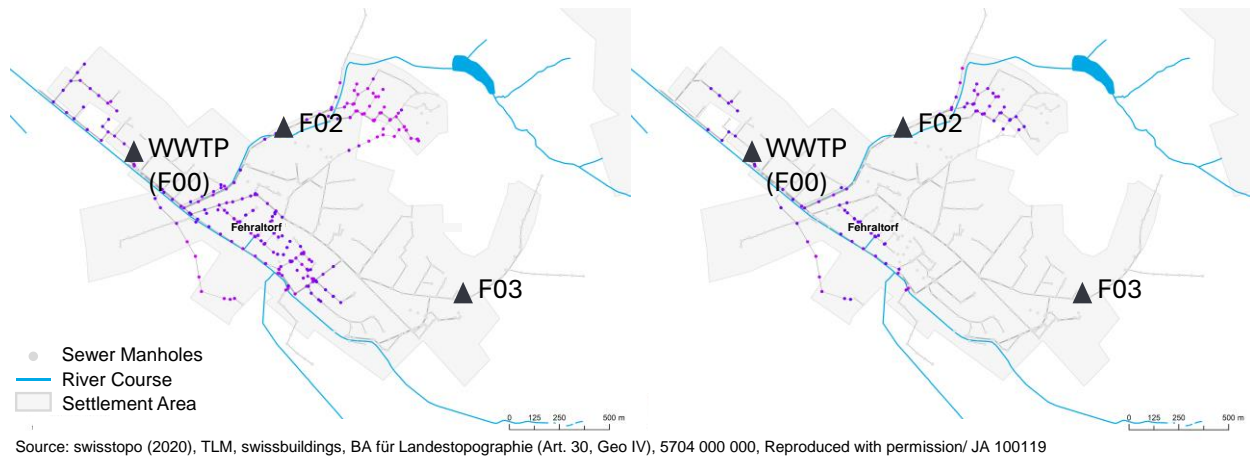


Figure S 46: Left: 256 sewer manholes in the Fehraltorf network are affected by groundwater in April 2018. The darker the color the more are manholes submerged in GW. Right: 100 sewer manholes in the Fehraltorf network are affected by groundwater in October 2018. The darker the color the more are manholes submerged in GW. ©Swisstopo (2020), TLM, swissbuildings, BA für Landestopographie (Art. 30 Geo IV), 5704 000 000, Reproduced with permission / JA 100119

S9.3 The value of redundant sensors in event-duration monitoring

S9.3.1.1 Problem Scope and Terminology

Assessing combined sewer overflows (CSOs) through tank level monitoring is crucial for quantifying pollution released into surface waters and optimizing sewer network operation. Long-term monitoring provides essential information to evaluate the significance of CSOs and mitigate their impact on the

environment and human health. Some countries have specific auto-surveillance protocols that require operators to submit monitoring data for legal compliance checks. In a few cases, this data is publicly accessible for transparent compliance assessment^{53 54}. The trend globally is to assess CSOs based on monitoring and various research initiatives have evaluated how different monitoring techniques can be used to assess pollution from CSOs (Gruber et al. 2005; Gamerith et al. 2009; Dirckx et al. 2011b; Sharma et al. 2014). Focusing on assessing the volume of CSO spills, Nickel & Fuchs (2020) analyzed real-world CSO data and found uncertainties in estimating overflow volumes based on level measurements. Nevertheless, they still consider it a valid method for quantifying spill volumes. Neglecting uncertainties in monitoring increases the risk of having useless or invalid data, which can compromise emission assessments and subsequent management actions.

S9.3.1.2 Approach

One strategy to reduce uncertainty in CSO spill monitoring is to install multiple sensors in a CSO structure, and use signal redundancy or signal diversity, to increase the reliability of overflow activity information, e.g. event duration monitoring. The UWO use case demonstrates the benefits of a dual-sensor approach, where overflow duration is independently monitored by two different types of sensors: an off-the-shelf ultrasonic sensor for continuous level monitoring and a capacitive sensor mounted at the weir crest (0, left). The capacitive sensor detects submergence and produces a binary "dry/wet" signal during overflow events. Figure S 47, right, illustrates the typical positioning of such a dual-sensor approach.

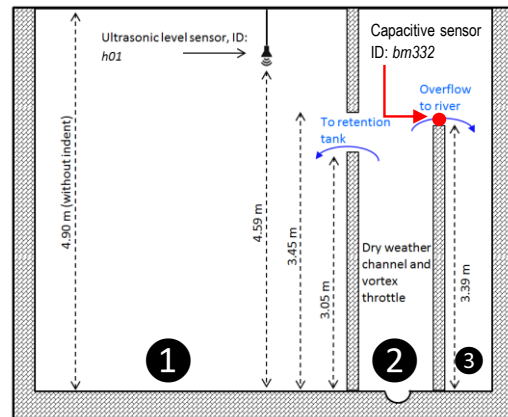


Figure S 47: Left: Capacitive sensor for overflow discharge detection at the weir crest basin RUB 59 after three years of operation. Photo: S. Bloem, Eawag. Right: Cross-section through overflow structure (not drawn to scale), including inflow chamber (2), retention tank (1), overflow to receiving water (3) and US level sensor (h01) and the capacitive sensors (bm332 and dl311).

S9.3.2 Results

Figure S 48 exemplary shows monitoring data of rainfall and its corresponding hydrological response - here: tank overflow - for a period of two days including two independent overflow events. In the given example, the dimensionless capacitive signal (▼) indicates a "wet" situation (weir crest overflow) for

⁵³ <https://opendatanetwork.herokuapp.com/dataset/data.ny.gov/ephi-ffu6> (data access 20.07.2023)

⁵⁴ <https://environment.data.gov.uk/dataset/21e15f12-0df8-4bfc-b763-45226c16a8ac> (data access 20.07.2023)

periods at which the monitored tank level (° – absolute water level) exceeds to height of the weir crest (-
-).

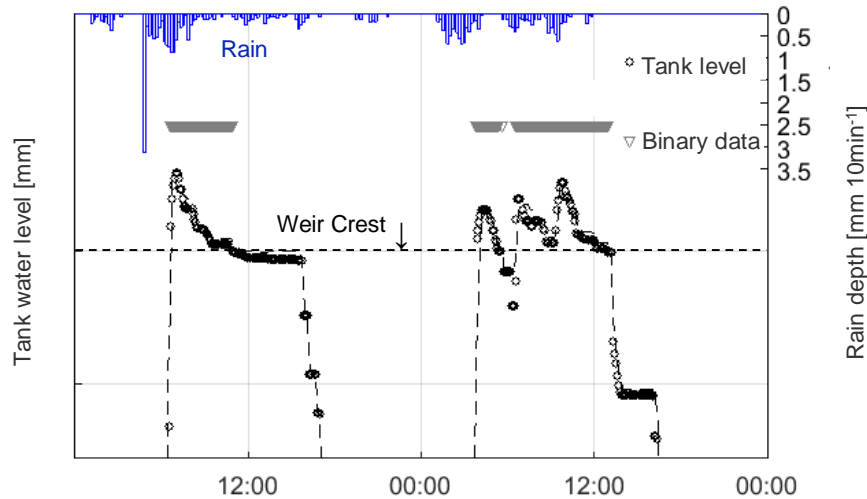


Figure S 48: Continuous tank water level (°) and binary information (derived from the capacitive sensor signal) reflecting the overflow activity for a period of two days for which two independent overflow events were recorded. Monitoring frequency is 5 minutes, for rainfall it is 1 minute.

The synchronized recordings in 0 demonstrate the chronological relationship between the data. However, they also expose slight discrepancies that can occur due to imperfect sensor calibrations. These discrepancies can lead to inaccurate quantification of overflow volumes, as observed in the study by Nickel & Fuchs (2020). By evaluating the capacitive sensor signal, which represents the "true" wet and dry information, alongside the level signal, confidence in the measured data is enhanced, and post-calibration of the level signal becomes possible.

Results in 0 illustrate the resulting differences on event-specific overflow durations 1) derived from level measurements (x-axis) and 2) from the di-electric signal (y-axis) before and after sensor calibration. Data reflect the activity of one and the same structure (RUB Morgenthal) for a period of 1077 days of operation for both sensors. A closer look reveals an obvious mismatch between overflow duration derived from (1) the tank level sensor and the (2) capacitive sensor (non-verified setting of the level sensor in the left chart in 0). Interesting to see that an incorrect offset settings at the level sensor can lead to significantly different overflow durations. The single ultrasonic sensor yields 12.69 d with overflows, which is ca. 50% less than the more reliable 25.62 d (Figure S 49). Relying solely on the level sensor, in this case, leads to a considerable underestimation of CSO activity.

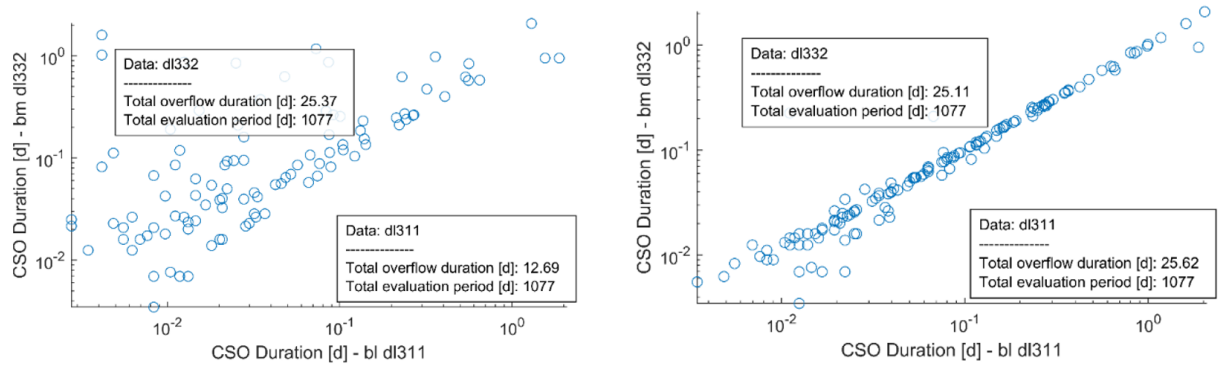


Figure S 49: Comparison of event-specific overflow durations derived from one capacitive sensors and one ultrasonic level sensor (dl311), prior (left) and after (right) correctly implementing the sensor settings.

S9.3.3 Conclusion

Application of two or more sensors of the same type provides the possibility to minimise measurement errors and increase data consistency through redundant recordings (cf. Bertrand-Krajewski et al., 2021). Based on our research with the parallel application of similar and diverse types of sensors (to monitor the same process), we can confirm this finding. Moreover, we find a considerable increase of robustness in the information on overflow activity, when assimilating recordings of two different types of sensors, i.e. data from level and dielectric conductivity (capacitive) sensors.

S9.4 The performance of a LoRaWAN network for underground applications

Sewer systems are crucial yet often under-monitored due to the lack of low-power wireless data transmission technology. LoRaWAN, a promising wireless communication technology that can operate over long distances, seems to be very promising for underground monitoring (Ebi et al., 2019). However, the performance of LoRaWAN networks in underground environments, particularly with metal-covered manholes and often harsh weather conditions, i.e. humidity and strong, widespread rainfall, remains uncertain. To address this issue, we evaluated the quality of service of the LoRaWAN network by comparing the Packet Error Rate (PER) of underground sewer nodes to those above ground. PER represents the percentage of data packets that fail to reach their destination due to transmission errors influenced by factors such as signal strength, interference, device distance, etc. In LoRaWAN networks, the network topology and device location can also affect the PER. We calculated the PER as an annual average of transmitted packages from all nodes in two groups based on their transmission intervals, one with a 1-min interval and another with a 5-min interval.

The results indicate a similar performance for all nodes (Table S4). With a PER of about 5%, the global average of data packet losses is very low. Median values indicate an even lower packet loss, i.e., 3 % during

Table S4: Summary statistics of the Quality of Service of the LoRaWAN wireless network. The mean of sensor median packet error rates (PER) was computed from weekly values for two groups of gateways (1min, 5min). While the global average of data packet losses is very low, i.e. approximately 5 %, median values indicate an even lower packet loss, i.e. 3 %. Also, the 1-minute nodes perform slightly better, most likely since a fair number of these nodes do not transmit from underground locations.

Median PER [-]	# of packets per week	2017 (# Sensors)	2018*	2019	2020	2021	2017 - 2021
1-min nodes	10080	0.026 (2)	0.020 (13)	0.058 (34)	0.048 (36)	0.037 (31)	0.050 (39)
5-min nodes	2016	0.056 (34)	0.043 (46)	0.055 (58)	0.061 (58)	0.032 (47)	0.056 (68)

most of the time. Interestingly, 1-minute nodes perform slightly better, most likely since a fair number of these nodes radio from aboveground locations.

In addition, we analysed the QoS (as inverse PER) on a weekly basis for all sensor nodes operated in the period from 2017 until May 2021. As expected, most nodes show a high QoS close to 1, while only a few nodes show a generally poor QoS, with a “minimum neck”, i.e. a narrow vertical stripe observed on the plot that shows a decrease in the QoS, such as *bm dl331* (0). Despite the occasional poor QoS for one or two weeks per year, e.g. *bl dl899* (0, top), the overall performance of these sensors for sewer monitoring

is not affected. As expected, sensor nodes locate above ground, e.g. those connected to a rain gauge (Figure S 50, light blue), have good data transmission. and do not show a “minimum neck”.

Future research can analyse the IoT radio network to explore LoRaWAN networks' potential for underground monitoring, advancing the maintenance of infrastructures such as heating, water, and electricity networks. Investigating environmental factors' impact, such as heavy rainfall or extreme temperatures, on key performance indicators, like RSSI or SNR ratio, as suggested by Blumensaat et al. (2017), could provide further insights into LoRaWAN networks' suitability for underground monitoring in challenging environments.

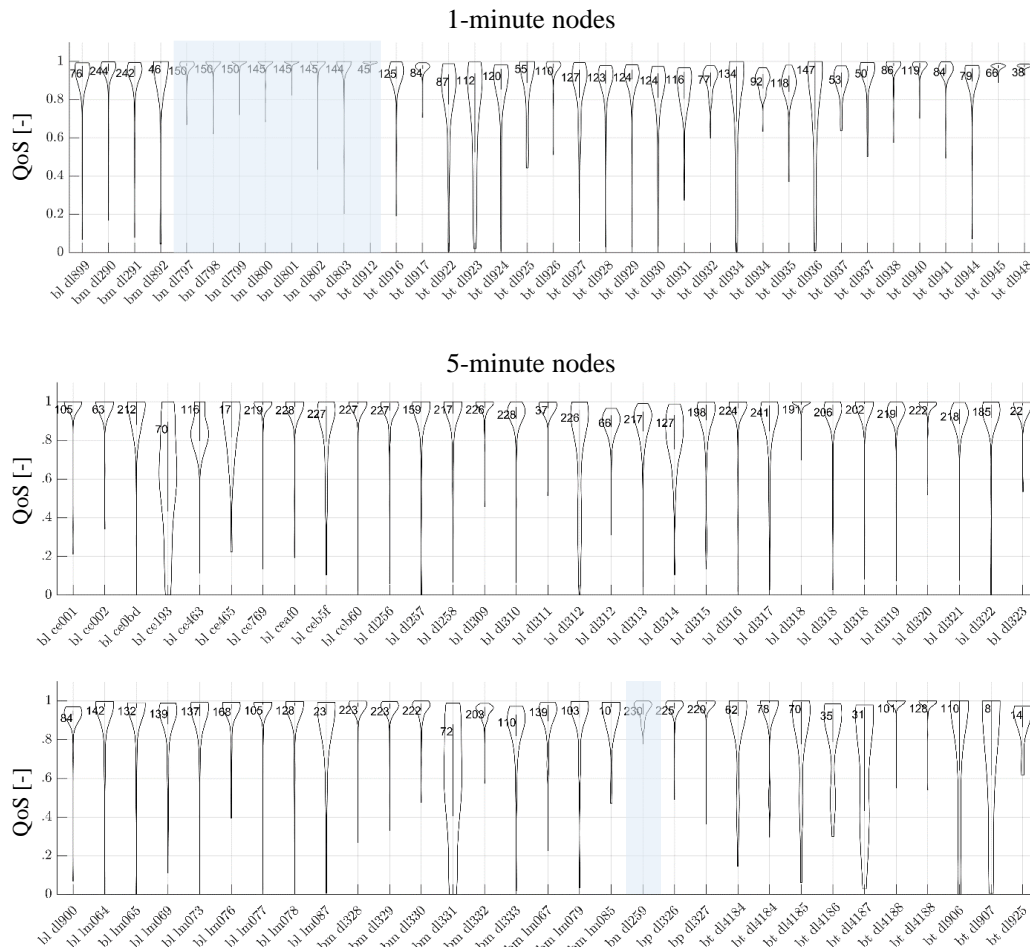


Figure S 50: Top: Distribution of QoS rates for 39 1-minute sensors (Jan 2017-May 2021). Arabic numbers show the number of weeks that a sensor had been in operation. Bottom: Distribution of QoS rates for 68 5-minute sensors. The more compact a cello shape and the closer the shape to 1, the higher the data transmission performance. For example, all “bn” sensor nodes, which transmit the observations from rain gauges above ground, show a very high performance.

S10 References

- Abdel-Aal, M., Villa, R., Jawiarczyk, N., Alibardi, L., Jensen, H., Schellart, A., Jefferson, B., Shepley, P., Tait, S., 2019. Potential influence of sewer heat recovery on in-sewer processes. *Water Sci. Technol. J. Int. Assoc. Water Pollut. Res.* 80, 2344–2351. <https://doi.org/10.2166/wst.2020.061>
- Aggarwal, C.C., 2017. *Outlier Analysis*. Springer International Publishing, Cham. <https://doi.org/10.1007/978-3-319-47578-3>
- Bertrand-Krajewski, J.-L., Clemens-Meyer, F.H.L.R., Lepot, M., 2021. Metrology in Urban Drainage and Stormwater Management: Plug and Pray. <https://doi.org/10.2166/9781789060119>
- Blumensaat, F., Ebi, C., Dicht, S., Rieckermann, J., Maurer, M., 2017. IoT driven low-power radio technology for highly distributed in-sewer monitoring – a data collection technique that shifts paradigms? in: 14th IWA/IAHR International Conference on Urban Drainage (ICUD 2017), 10.-15.09.2017. Presented at the ICUD 2017, Czech Republic. <https://www.dora.lib4ri.ch/eawag/islandora/object/eawag:24439>
- Boebel, M., Frei, F., Blumensaat, F., Ebi, C., Meli, M. L., and Rüst, A.: Batteryless Sensor Devices for Underground Infrastructure—A Long-Term Experiment on Urban Water Pipes, *Journal of Low Power Electronics and Applications*, 13, 31, <https://doi.org/10.3390/jlpea13020031>, 2023.
- Branisavljević, N., Prodanović, D., Pavlović, D., 2010. Automatic, semi-automatic and manual validation of urban drainage data. *Water Sci. Technol.* 62, 1013. <https://doi.org/10.2166/wst.2010.350>
- Deheer, K., 2022. A Look Behind Using Machine Learning for Anomaly Detection. URL <https://www.trinnex.io/insights/a-look-behind-using-machine-learning-for-anomaly-detection> (accessed 4.19.23).
- Deb, K., Pratap, A., Agarwal, S. and Meyarivan, T. (2002) A fast and elitist multiobjective genetic algorithm: NSGA-II. *IEEE Transactions on Evolutionary Computation* 6(2), 182-197. <https://doi.org/10.1109/4235.996017>
- Dirckx, G., Thoeve, Ch., De Gueldre, G., Van De Steene, B., 2011. CSO management from an operator's perspective: a step-wise action plan. *Water Sci. Technol.* 63, 1044–1052. <https://doi.org/10.2166/wst.2011.288>
- Rieckermann, J., A. Disch, 2022. Challenges and Prospects in Anomaly Detection of Sewer Monitoring Data: Annotating Synthetic Sewer Data with Known Sensor Failures. Pre-print. <https://doi.org/10.31224/3520>
- Ebi, C., Schaltegger, F., Rust, A., Blumensaat, F., 2019. Synchronous LoRa mesh network to monitor processes in underground infrastructure. *IEEE Access* 7, 57663–57677. <https://doi.org/10.1109/ACCESS.2019.2913985>
- Elías-Maxil, J.A., Hofman, J., Wols, B., Clemens, F., van der Hoek, J.P., Rietveld, L., 2017. Development and performance of a parsimonious model to estimate temperature in sewer networks. *Urban Water J.* 14, 829–838. <https://doi.org/10.1080/1573062X.2016.1276811>

- Figueroa, A., Hadengue, B., Leitão, J., Rieckermann, J., Blumensaat, F., 2021. A distributed heat transfer model for thermal-hydraulic analyses in sewer networks. *Water Res.* 117649 (11 pp.). <https://doi.org/10.1016/j.watres.2021.117649>
- Fraternali, P., Castelletti, A., Soncini-Sessa, R., Vaca Ruiz, C., Rizzoli, A.E., 2012. Putting humans in the loop: Social computing for Water Resources Management. *Environ. Model. Softw.* 37, 68–77. <https://doi.org/10.1016/j.envsoft.2012.03.002>
- Gamerith, V., Muschalla, D., Könnemann, P., Gruber, G., 2009. Pollution load modelling in sewer systems: an approach of combining long term online sensor data with multi-objective auto-calibration schemes. *Water Sci. Technol.* 59, 73–79. <https://doi.org/10.2166/wst.2009.772>
- Gruber, G., Winkler, S., Pressl, A., 2005. Continuous monitoring in sewer networks an approach for quantification of pollution loads from CSOs into surface water bodies. *Water Sci. Technol.* 52, 215–223. <https://doi.org/10.2166/wst.2005.0466>
- Hadengue, B., Joshi, P., Figueroa, A., Larsen, T.A., Blumensaat, F., 2021. In-building heat recovery mitigates adverse temperature effects on biological wastewater treatment: A network-scale analysis of thermal-hydraulics in sewers. *Water Res.* 204, 117552. <https://doi.org/10.1016/j.watres.2021.117552>
- Hager, W.H., 1999. *Wastewater hydraulics: Theory and practice*. Springer, Berlin.
- Hastie, T., Tibshirani, R., Friedman, J., 2009. *The elements of statistical learning: Data mining, inference, and prediction*, 2. ed. ed, Springer series in statistics. Springer, New York and NY.
- Hunziker-Betatech AG (2014). *VGEP Fehraltorf-Russikon*. Hunziker-Betatech AG, Winterthur, 2014.
- Hunziker-Betatech AG (2016). *GEP Fehraltorf*. Hunziker-Betatech AG, Winterthur, 2016.
- Huisman, J.L., 2001. *Transport and transformation processes in combined sewers*. ETH Zürich.
- P. Joshi, J.P. Leitão, M. Maurer, P.M. Bach (2021). Not all SuDS are created equal: impact of different approaches on combined sewer overflows. *Water Res.*, 191. <https://doi.org/10.1016/j.watres.2020.116780>
- Kerkez, B., Gruden, C., Lewis, M., Montestruque, L., Quigley, M., Wong, B., Bedig, A., Kertesz, R., Braun, T., Cadwalader, O., Poresky, A., Pak, C., 2016. Smarter Stormwater Systems. *Environ. Sci. Technol.* 50, 7267–7273. <https://doi.org/10.1021/acs.est.5b05870>
- Moriasi, D. N., Arnold, J. G., Van Liew, M. W., Bingner, R. L., Harmel, R. D., & Veith, T. L. (2007). Model evaluation guidelines for systematic quantification of accuracy in watershed simulations. *Transactions of the ASABE*, 50(3), 885-900. <http://dx.doi.org/10.13031/2013.23153>
- Nickel, J.P., Fuchs, S., 2020. Qualitative Untersuchung von Mischwasserentlastungen in Bayern: Schlussbericht. <https://doi.org/10.5445/IR/1000137305>
- Ramgraber, M., Weatherl, R., Blumensaat, F., Schirmer, M., 2021. Non-Gaussian Parameter Inference for Hydrogeological Models Using Stein Variational Gradient Descent. *Water Resour. Res.* 57, e2020WR029339. <https://doi.org/10.1029/2020WR029339>
- Rodriguez Bennadji, M.: The influence of Green Infrastructure on the resilience of urban drainage systems, 2022. <https://ore.exeter.ac.uk/repository/handle/10871/131516>

- Rodriguez, M., Fu, G., Butler, D., Yuan, Z., and Cook, L., 2023: Global resilience analysis of combined sewer systems under continuous hydrologic simulation, *Journal of Environmental Management*, 344, 118607, <https://doi.org/10.1016/j.jenvman.2023.118607>.
- Ruggaber, T.P., Talley, J.W., Montestruque, L.A., 2007. Using Embedded Sensor Networks to Monitor, Control, and Reduce CSO Events: A Pilot Study. *Environ. Eng. Sci.* 24, 172–182. <https://doi.org/10.1089/ees.2006.0041>
- Russo, S., Besmer, M.D., Blumensaat, F., Bouffard, D., Disch, A., Hammes, F., Hess, A., Lürig, M., Matthews, B., Minaudo, C., Morgenroth, E., Tran-Khac, V., Villez, K., 2021. The value of human data annotation for machine learning based anomaly detection in environmental systems. *Water Res.* 206, 117695. <https://doi.org/10.1016/j.watres.2021.117695>
- Schmitt, T. G., Becker, M., Flores, C., Pfeiffer, E., Sitzmann, D., and Uhl, M. (2008). "Modellkalibrierung zur Qualitätssicherung von Kanalnetzberechnungen." (in German). *Korrespondenz Abwasser*, 55(12), 1306-1313.
- Sharma, A. K., Lynggaard-Jensen, A., Vezzaro, L., Andersen, S. T., Brodersen, E., Eisum, N. H., Snediker Jacobsen, B., Høgh, J., Gadegaard, T. N., Mikkelsen, P. S., & Rasmussen, M. R. (2014). Advanced Monitoring of Combined Sewer Overflows: what to measure and how to measure. In *Proceedings of the 13th International Conference on Urban Drainage*.
- Staufner, P., Scheidegger, A., Rieckermann, J., 2012. Assessing the performance of sewer rehabilitation on the reduction of infiltration and inflow. *Water Res.* 46, 5185–5196. <https://doi.org/10.1016/j.watres.2012.07.001>
- US EPA, 2021. Smart Data Infrastructure for Wet Weather Control and Decision Support, March 2021.
- Wani, O., Scheidegger, A., Carbajal, J.P., Rieckermann, J. and Blumensaat, F. (2017) Parameter estimation of hydrologic models using a likelihood function for censored and binary observations. *Water Research* 121, 290-301. <https://doi.org/10.1016/j.watres.2017.05.038>